Increasing summer net CO_2 uptake in high northern ecosystems inferred from atmospheric inversions and remote sensing

Lisa R. Welp[1,*], Prabir K. Patra[2], Christian Rödenbeck[3], Rama Nemani[4], Jian Bi[1], Stephen C. Piper[1], and Ralph F. Keeling[1]

[1]Scripps Institution of Oceanography, University of California San Diego, La Jolla, California, USA

[2]Agency for Marine-Earth Science and Technology, Yokohama, Japan

[3]Max Planck Institute for Biogeochemistry, Jena, Germany

[4]NASA Ames Research Center, Moffet Field, California, USA

*now at: Purdue University, West Lafayette, IN, USA

Correspondence to: L. R. Welp (lwelp@purdue.edu)

Abstract. Warmer temperatures and elevated atmospheric CO_2 concentrations over the last several decades have been credited with increasing vegetation activity and photosynthetic uptake of CO_2 from the atmosphere in the high northern latitude ecosystems: the boreal forest and Arctic tundra. At the same time, fire frequency and severity are increased, and some regions of the boreal forest show signs of stress due to drought or insect disturbance. The recent trends in net carbon balance of these ecosystems, across heterogeneous disturbance patterns, and the future implications of these changes are unclear. Here we examine CO_2 fluxes from northern boreal and tundra from 1986 to 2012 estimated from two inverse models (RIGC and Jena), both using measured atmospheric CO_2 concentrations and wind-fields from interannually variable reanalysis. In the arctic zone, the latitude region above 60°N excluding Europe (10°W – 63°E), neither model finds a significant long-term trend in annual CO_2 balance. The boreal zone, the latitude region from approximately 50°N to 60°N, again excluding Europe, absorbed an extra 8–11 Tg C yr^{-1} over the period from 1986 to 2006, resulting in an annual CO_2 sink in 2006 that was 170–230 Tg C larger than in 1986. This same trend appears to continue through 2012 as well. In both latitudinal zones, the seasonal amplitude of monthly CO_2 fluxes increased due to increased uptake in summer, and in the arctic zone, also due to increased fall CO_2 release. Both models showed a seasonal flux amplitude increase of nearly 1% yr^{-1} in the arctic zone, over twice the trend in the boreal zone fluxes. These findings suggest that the boreal zone has been maintaining and likely increasing CO_2 sink strength over this period, despite browning trends in some regions, changes in fire frequency and land use. Meanwhile the arctic zone shows increased summer CO_2 uptake, consistent with strong greening trends, is offset by increased fall CO_2 release, resulting in a net neutral trend in annual fluxes. The inversion fluxes from the arctic and boreal zones covering the permafrost regions showed no indication of a large-scale positive climate-carbon feedback caused by warming temperature on high northern latitude terrestrial CO_2 fluxes as of 2012.

1 Introduction

The high northern latitudes, including the tundra and boreal forest regions, are particularly vulnerable to the effects of climate change as this region has been experiencing dramatic changes in recent climate. Warming in northern ecosystems results in many physical and ecological changes that have consequences

5   for carbon cycling (Chapin, 2005; Hinzman et al., 2005; McGuire et al., 2009; Serreze et al., 2000; Walther, 2010). Annual mean surface air temperatures over land increased by 0.64°C per decade north of 60°N from 1979 to 2008, roughly twice the rate of 0.33°C per decade for the northern hemisphere as a whole (ACIA, 2004; Bekryaev et al., 2010). This northern amplification has been attributed to ice/snow-albedo feedbacks (Cess et al., 1991; Qu and Hall, 2007; Serreze and Barry, 2011). Minimum sea ice extent

10   in the Arctic Ocean has declined rapidly (Comiso et al., 2008) with feedbacks and teleconnections on the continental areas as well (Francis et al., 2009). Impacts in the northern regions are predicted to intensify, as climate scenario modeling projects further arctic temperature increases of 5–7 °C by the end of this century (ACIA, 2004) and atmospheric CO_2 concentrations continue to rise at a rate approaching 2.0 ppm per year.

Tundra ecosystems and boreal forests hold large stores of carbon in soil organic matter buried in cold or

15   frozen permafrost soils. It is estimated that 1,400 to 1,850 Pg C are stored in high northern latitude soils and another 60 to 70 Pg C in above and below-ground vegetation (McGuire et al., 2009). The natural turnover time of this carbon is very slow, but there is a risk that warmer temperatures will increase microbial respiration rates and expose previously frozen organic matter to decomposition by melting the permafrost (Schuur et al., 2008). Over the past several decades there has been a measureable trend to earlier

20   spring snowmelt and surface soil thaw (McDonald et al., 2004; Smith, 2004) and increases in permafrost borehole temperatures (Romanovsky et al., 2010) demonstrating changes in the thermal stability of northern circumpolar soils. It has been speculated that warming could trigger massive release of carbon from these soils, in the form of CO_2 and CH_4, leading to a positive climate-carbon feedback (Schuur et al., 2008). This has been nicknamed the Arctic 'carbon bomb' in the popular media.

25   However, warming and the associated lengthening of the growing season encourages plant growth in these otherwise temperature-limited areas, as does increased atmospheric CO_2 fertilization (Lloyd and Farquhar, 1996) and increased nitrogen deposition (Holland et al., 1997). The net carbon balance of increased plant growth and increased soil respiration is unclear, but has important consequences for predicting carbon-climate feedbacks.

30   Measurements of atmospheric CO_2 concentrations at Barrow, Alaska by Keeling et al. (1996) provided evidence for increased photosynthetic activity and net primary production (NPP) at northern latitudes from 1960 through 1994. The changes were attributed to increased CO_2 uptake by vegetation during spring and summer, leading to earlier drawdown and larger seasonal amplitudes of atmospheric CO_2 concentrations (Keeling et al., 1996; Randerson et al., 1999). This perspective is also supported by satellite observations

35   of an increase in vegetation greenness at northern latitudes (1997) and global ecosystem process models

suggesting that northern ecosystems have become more productive as a result of combined changes in temperature, CO_2 concentration and nitrogen availability (Kimball et al., 2007; McGuire et al., 2001). An updated perspective on the northern CO_2 cycles from Barrow data and from repeated airborne surveys of the mid troposphere showed 50% increase in the amplitude from 1960 to 2010, implying a significant

5   increase in northern ecosystem growing season CO_2 uptake over the last several decades (Graven et al., 2013).

Since the late 1990s, however, some indicators of ecosystem function suggest that the terrestrial biosphere response to recent climate change in the high northern latitudes may be different from the previous few decades, and that terrestrial CO_2 uptake has since slowed down or even turned to a net source. Analysis of

10   the changes in the seasonality of atmospheric CO_2 suggests that temperature-induced late summer drought may be increasing fall CO_2 release and offsetting enhanced spring CO_2 uptake (Angert et al., 2005; Piao et al., 2008).   Piao et al. (2008) estimated that current warming during autumn increases respiration in northern ecosystems enough to cancel 90% of the increased spring CO_2 uptake. While these studies provide important insights into changing ecosystem function, changes in CO_2 seasonal cycles in the

15   atmosphere depend not just on surface fluxes but also variations in atmospheric circulation (Higuchi, 2002).

Vegetation productivity and distribution has also changed during this same period. The treeline has advanced northward and woody shrub colonies have expanded in the tundra zone displacing less productive species (Goetz et al., 2005; Lloyd et al., 2005; Pearson et al., 2013; Sturm, 2005; Tape et al., 2006). Within

20   the boreal zone, satellite observations show large areas of the boreal forest not disturbed by fire have been 'browning' since 2000 as observed by Normalized Difference Vegetation Index (NDVI) measurements (Goetz et al., 2005; 2007; Verbyla, 2008; 2011; Zhang et al., 2008). One statistical analysis suggests the browning trends in the Alaskan boreal forest have been ongoing for the last three decades (Forkel et al., 2013). These results have been consistent with ground observations which also report widespread tree

25   mortality caused by insect outbreaks due to warmer winter temperatures (Kurz et al., 2008) and drought (Hogg et al., 2008; Peng et al., 2011). However, an updated NDVI processing algorithm in the NDVI3g product shows overall more areas greening than the older version, with the largest greening in western Eurasia and some more areas of browning in North America (Xu et al., 2013).

It is important to determine the net carbon balance of these large northern regions to see if they have been

30   increasing or decreasing in CO_2 sink strength, or perhaps transitioning to a net CO_2 source. Approaches used to estimate the net CO_2 fluxes of large areas include forest inventories, atmospheric inversions, and process-based models. Each of these methods has its strengths and weaknesses. Atmospheric inversions can infer the global, continental and sometimes regional-scale fluxes of CO_2 between the atmosphere and the land biosphere and the oceans, by analyzing the temporal and spatial records of atmospheric CO_2

35   change (Enting, 2002). Inversions have the advantage of including the effects of disturbance, but are

limited to the period of sufficient CO_2 concentration observations and are best suited to resolving continental-scale fluxes. Few inversion analyses have specifically focused on the high northern latitude terrestrial ecosystems. Zhang et al. (2013) aggregated the inversion fluxes from five different models into Eastern Canada and Western Canada plus Alaska. This study found consistency in the trends between

5   inversions and increasing CO_2 uptake in Eastern Canada and no long-term trend in Western Canada plus Alaska.

Forest inventories are not suited to quantifying changes in below-ground carbon, therefore they are hard to compare directly to atmospheric inversion results. They are better at identifying spatially variable trends in forest productivity. One study found no trend in above-ground carbon stocks in Eastern Canada, but did

10   find drought-induced carbon losses in Western Canada (Hogg et al., 2008; Ma et al., 2012; Michaelian et al., 2010; Peng et al., 2011). Process-based modeling studies attempt to account for above and below-ground carbon changes while providing full spatial coverage, and are therefore capable of simulating net ecosystem fluxes that can be compared to atmospheric inversions. Several studies have concluded that the Arctic tundra and boreal forests have been decreasing sinks or increasing sources since the 1980s due to

15   climate effects, namely warmer temperatures increasing soil organic matter decomposition, and increased fire and insect disturbance, offsetting increased CO_2 uptake driven by CO_2 fertilization (Bradshaw and Warkentin, 2015; Hayes et al., 2011; McGuire et al., 2010).

Here we focus on trends in the carbon uptake of the land biosphere north of approximately 50°N. We examine large regional-scale variability in terrestrial CO_2 fluxes from two atmospheric inversions using

20   interannually variable atmospheric transport from 1985 to 2012. One objective of this study is to evaluate temporal changes in the annual and seasonal land biosphere CO_2 fluxes. We determine in what months surface CO_2 fluxes have changed, i.e. increased summer uptake or winter release. We further examine NDVI and air temperature trends and correlations to provide some spatial and process context for changes in the temporal fluxes from the inversions.

25   **2 Methods and data analysis**
2.1 Inversion models

We compared two different atmospheric inversions: the RIGC inversion and the Jena CO_2 inversion (s85v3.6). The RIGC inversion method was adapted from Rayner et al. (1999), and largely followed the TransCom-3 protocol (Gurney et al., 2003). The RIGC model uses a 64-region time-dependent inverse

30   method to infer carbon source/sink estimates based on the method of Patra et al. (2005). The RIGC inverse calculation starts with *a priori* fossil-fuel emissions and terrestrial and oceanic fluxes which are then optimized to match observations. Total anthropogenic CO_2 emissions were derived from the Oak Ridge National Lab monthly fossil fuel estimates (Boden et al., 2009) plus bunker fuel and non-fuel oxidation estimates from the Emissions Database for Global Atmospheric Research (EDGAR) (Oliver and

35   Berdowski, 2001). It uses the NIES/FRCGC (National Institute for Environmental Studies/Frontier

Research Center for Global Change) global forward transport model driven by interannually varying (IAV) meteorology from the NCEP reanalysis and the GLOBALVIEW-CO_2 data product to derive residual *a posteriori* land and ocean surface fluxes for the 64 inversion regions. The focus is primarily on the interannual variability in the CO_2 fluxes which is considered more robust than the long-term mean flux (Baker et al., 2006).

In the RIGC inversion, the GLOBALVIEW-CO_2 input was limited to the 26 CO_2 observation stations, which have nearly continuous records over the period (Table 1). Among these are stations that document changes in high northern latitudes, including Barrow (71°N), Alert (82°N), Station M (66°N), Cold Bay Alaska (55°N), Shemya (52°N), and Cimone (44°N). A selected set of stations was used to avoid creating spurious trends in the inversion results from adding new stations mid-way through the inversion period. All selected stations had at least 71% temporal coverage and came online by 1989. Stations north of 39°N had 84% to 100% temporal coverage.

Compared to the RIGC model, the Jena inversion, version s85_v3.6 (Rodenbeck, 2005), uses a slightly different set of 19 stations selected to completely cover the 1985–2012 estimation period, but includes all of the same stations north of 50°N (Table 1). It uses individual measurements from various sampling networks, without smoothing or gap filling. Fluxes are estimated at the grid-scale resolution (approximately 4° latitude by 5° longitude), to reduce aggregation errors. However, to counteract that the estimation would be underdetermined, spatial and temporal a-priori correlations are imposed, smoothing the estimated flux field on scales smaller than about 1 week and about 1600 km (land, in longitude direction), 800 km (land, latitude), 1900 km (ocean, longitude), or 950 km (ocean, latitude), respectively. Land flux adjustments are spatially weighted with a productivity proxy (long-term mean NPP from the LPJ model). Prior fluxes comprise anthropogenic CO_2 emissions from EDGAR v4.2 (EDGAR, 2011), a constant spatial flux pattern on land (time-mean NEE from the LPJ model), and a mean seasonal cycle on the ocean (ocean-interior inversion by Mikaloff Fletcher et al. (2006)), with seasonality from Takahashi et al. (2002). The Jena inversion uses the TM3 global atmospheric transport model driven by meteorology from the NCEP reanalysis. The gridded *a posteriori* land and ocean surface fluxes are aggregated to our analysis regions. Resulting fluxes are valid from 1985 to 2012.

2.2 Datasets

We compared CO_2 fluxes with satellite-based normalized difference vegetation index (NDVI) data over the same time period and with land temperature records. NDVI is a proxy for photosynthetically active above-ground biomass. We use NDVI data produced by NASA's Global Inventory Modeling and Mapping Studies (GIMMS version 3g) from measurements of the Advanced Very High Resolution Radiometer satellite and supplied at the monthly, 1 x 1 degree resolution (Pinzon and Tucker, 2014). Winter NDVI data was excluded from this analysis because of the confounding influence of snow (Myneni et al., 1997). We

defined growing season NDVI (Zhou et al., 2001) as the sum of monthly NDVI from April to October following the example of earlier work.

We used monthly mean temperature anomalies from the NASA GISS 2 x 2 degree gridded dataset to compare to CO_2 fluxes and NDVI variability (Hansen et al., 1999). Temperature anomalies are computed by subtracting the 1951 to 1980 mean. Throughout this manuscript, we abbreviate seasonal means by 'MAM' (March, April, May), `JJA' (June, July, August), `SON' (September, October, November), and `DJF' (December, January, February).

We examined estimates of fire CO_2 emissions from 1985 to 2000 from the RETRO compilation and from 1997 to 2012 from the GFEDv4 model (Giglio et al., 2013; Schultz et al., 2008).

2.3 Analysis approach

We focused our analysis on land carbon fluxes in two roughly zonal bands at high northern latitudes partly based on the TransCom regional boundaries defined by Gurney et al. (2003). Figure 1 shows the regions of Boreal Asia (BA) and Boreal North America (BNA) that we aggregated into what we refer to as the 'boreal zone' roughly between 50°N and 60°N and the 'arctic zone' north of 60°N. Note here that while we refer to the boreal zone as roughly '50°N to 60°N', the southern boundary is not defined at the 50°N latitude, but follows the irregular southern boundary of boreal forest (stippled area in Fig. 1). We decided to omit the European (EU) land region from our zonal analysis for two reasons. First, the TransCom protocol followed by the RIGC inversion does not separate northern Europe at 60°N like it does for BA and BNA, rather northern EU section is everything north of 50°N. Second, the EU region includes a relatively small fraction of the tundra and boreal forest ecosystems compared to BA and BNA, and the forest area is highly managed. Our focus is how the less intensively managed ecosystems of the north have been responding to climate change and examining the boreal zone and the arctic zone should maximize any potential signals of change. A similar approach of excluding EU was used in the Arctic analysis of McGuire et al. (2009).

The atmospheric inversion approach with relatively sparse atmospheric CO_2 concentration observations starting in the 1980s is most strongly constrained in the latitudinal direction reflecting the rapid atmospheric mixing of a few weeks around latitude circles. For that reason, we check the EU and Northern Ocean (NO) regions for any trends that might be offsetting trends in what we define as the 'Boreal zone' and the 'Arctic zone' caused by spatial errors in the assignment of surface fluxes by the inversion analyses that could complicate our interpretations of the data. We performed the trend analysis for two periods: from 1986-2006 when we have inversion results for both models, and from 1985–2012 for just the Jena s85 inversion.

We examine trends in the monthly, seasonal, and annual net ecosystem exchange (NEE) fluxes from the inversion models. Amplitudes of the annual seasonal cycle in CO_2 fluxes were calculated from the

maximum and minimum monthly mean fluxes within each calendar year as: flux amplitude = maximum NEE - minimum NEE.

The flux amplitude is indirectly related to the amplitude in atmospheric CO_2 concentrations, as the atmospheric concentration is roughly the integral of the monthly fluxes. It is unnecessary to detrend the

5   time series of fluxes from the models prior to calculating the flux amplitude, unlike the concentration amplitude. We also examine the latitudinal gradient of the trends in the seasonal fluxes in ~4° latitude bands from the gridded Jena inversion. This analysis was not possible with the RIGC inversion because of the larger basis regions. This approach attempted to answer the question of whether summer uptake is increasing or fall respiration (or both) and how that might change with latitude.

10   ## 3 Results
3.1 CO_2 flux trends
3.1.1 Arctic zone (>60°N)

The arctic zone containing the tundra region showed no significant trend in annual CO_2 uptake (Fig 2a, Table 2) from 1986–2006 in either inversion. The longer period, 1985–2012, in the Jena inversion did

15   show a small but significant trend toward increased uptake of an extra 4 Tg C yr^{-1}. Anomalously strong annual CO_2 uptake occurred in years 1990 and 2004 in the RIGC inversion and strong CO_2 release in 1996. These large anomalous fluxes were not present in the Jena inversion.

The Jena and RIGC inversions differ in their mean seasonal cycle in the arctic zone, with the RIGC inversion yielding peak CO_2 uptake approximately twice that of the Jena inversion (Fig 3b). Trends in

20   monthly net CO_2 flux, computed with the method of Randerson et al., (1997), reveal increasing uptake in July in both inversions and stronger releases in September, October, and November (Fig. 3d). These seasonal changes largely cancel in the annual net fluxes, but contribute to increasing CO_2 flux amplitudes, computed as the difference between the maximum and minimum monthly CO_2 fluxes, by ~1.0% year^{-1} relative to the mean seasonal amplitude from 1986 to 2006 for both inversions (Fig 4, Table 2). Figure 5

25   shows the annual values of the July CO_2 flux in Pg C yr^{-1} over this record. This is directly related to July trend data in Figure 3d. On a per area basis, this translates to an increase in July peak summer CO_2 uptake of 0.007–0.013 gC m^{-2} day^{-1} yr^{-1}, depending on the inversion used, averaged over the entire zone or a ~10% increase in peak summer CO_2 uptake over these 21 years. The trends over 1985–2012 are similar at 0.007 gC m^{-2} day^{-1} yr^{-1} for the Jena inversion (Table 2).

30   #### 3.1.2 Boreal zone (50°N – 60°N)

The boreal zone shows a trend towards increasing annual net CO_2 uptake in both inversions (Fig 2b, Table 2). From 1986 to 2006, the trend in the RIGC inversion was 10 Tg C yr^{-1} with a p-value <0.1. The Jena inversion resulted in a similar trend of 8 Tg C yr^{-1}, but did not meet the criteria for significance, p>0.1

(Table 2). The most noticeable difference between the inversions is that the RIGC inversion predicted an anomalous release of CO_2 in 1994 that was not confirmed by the Jena inversion. Over the longer period from 1985–2012, the Jena inversion predicts the same trend toward greater CO_2 uptake with a slope of 7–8 Tg C yr^{-1} and a p-value <0.1 (Fig. 2b, Table 3).

5 The Jena and RIGC inversions resulted in similar mean seasonal cycles of the monthly net CO_2 fluxes, but the seasonal amplitude in the Jena inversion was slightly larger (Fig. 3a). The trends in the monthly fluxes show increasing CO_2 uptake in the growing season, and in the case of the Jena inversion, increasing CO_2 uptake in the spring and release in the fall (Fig. 3c). There was a corresponding increase in the seasonal amplitude of net CO_2 flux of 0.4% yr^{-1} (p=0.04) estimated by the Jena inversion, but not in the RIGC

10 inversion (Fig. 4b and Table 2). Figure 5 shows the time series CO_2 flux in July (month of peak flux) over this period. Both models show an increase in July CO_2 uptake although they don't agree on anomalies from year to year. In Figure 3cd, both models also show an increase in the fall CO_2 release in the northern land regions, but the Jena inversion attributes this mostly to the boreal zone, whereas the RIGC inversion attributes it mostly to the arctic zone.

15 **3.2 Europe and Northern Ocean fluxes and fossil-fuel emissions**

For completeness, we also show the time series of CO_2 flux trends, both net annual and seasonal amplitude from the 55°N to 80°N region of Europe (EU) and the northern ocean (NO) to be sure that fluxes in these regions are not compensating for fluxes in our analysis of the BA+BNA regions (Fig. 6). There were no offsetting positive trends in the annual net flux of CO_2 or negative trends in the seasonal amplitude in EU

20 from 1986–2006 and none were statistically significant (Table 2). Likewise the NO flux trends are insignificant with the exception of the seasonal amplitude trend in the RIGC inversion of -2.4% yr^{-1}. This was statistically significant using the modified Mann-Kendall p-test, but the mean amplitude of the ocean flux (~0.1 Pg C yr^{-1}) is much too small to offset gains in the land flux amplitude in the BA+BNA regions (mean 4.6–9.9 Pg C yr^{-1} for north of 60°N and mean 11.4–13.9 Pg C yr^{-1} for 50°N–60°N). There is no

25 indication that inversion-resolved trends in the EU and NO regions in the north of 50°N zone are forcing offsetting trends in the BA+BNA regions, however, we cannot rule out misallocation of fluxes among the inversion regions used in this study.

The RIGC and Jena inversions use different fossil-fuel emissions datasets to isolate the net land surface fluxes related to biology. Comparing fossil-fuel emissions for the EU and BA+BNA Arctic and Boreal

30 zones used in each inversion (SI Fig. 1) shows that while the mean emissions were lower in the RIGC inversion, the IAV and trends in absolute fluxes were similar in each inversion. Differences in the fossil emissions are therefore unlikely to contribute significantly to trends in the biological land fluxes of the BA+BNA Arctic and Boreal zones.

3.3 Flux amplitude trends

We define the seasonal flux amplitude as the difference between the peak summer CO_2 uptake and the maximum CO_2 release in the fall, within a calendar year. We examined changes in the flux amplitude using several approaches. Figure 4 shows that the flux amplitude increase, in percent of the mean flux amplitude, is larger in the Arctic zone than the Boreal zone. This is also reflected in the monthly trends in Figure 3cd.

We also examined the change in the seasonal flux amplitude across latitudes from the Jena inversion to see if this observed increase in the seasonal flux amplitude was unique to the high northern latitudes, or if it is more widespread. Here we define the fall flux as the mean of SON, and the summer uptake is fixed as July. Figure 7 shows that significant increases in the annual flux amplitude have occurred between 40–70°N with a peak from 50–65°N. Looking at the fall and summer contributions separately shows that both increasing fall CO_2 release and peak summer uptake contribute to the annual amplitude increase, with increasing fall CO_2 release outpacing peak summer uptake in the 40–50°N band and increasing peak summer CO_2 uptake outpacing fall release in the 55–65°N band.

3.4 Fire emissions

The net fluxes examined here are dominated by land biosphere fluxes, but they also include CO_2 emissions from forest fires, which occur mostly in summer (Fig. S3) (van der Werf et al., 2006). If fire activity were responsible for the trend in summer net carbon uptake, then fire frequency would need to be decreasing. We examined estimates of fire CO_2 emissions from 1985 to 2000 from the RETRO compilation and from 1997 to 2012 from the GFEDv4 model (Giglio et al., 2013; Schultz et al., 2008). While we cannot combine the two emissions estimates into a continuous time series because of the different methodologies used, we can examine trends over each record. Neither record shows evidence of decreasing fire emissions over their respective time periods (Fig. S4), therefore, biological activity clearly dominates the trends.

3.5 Temperature and NDVI trends

In order investigate possible drivers of the trends in CO_2 fluxes, we also examine trends in surface air temperature and NDVI. Seasonal temperature changes from 1986 through 2006 were not uniform across the far north (Fig. 8). In general, warming has been the greatest in the fall (SON) and winter (DJF), although these patterns vary regionally. Despite the general trend toward warming, cooling trends are seen over the 1986–2006 period for Siberia in winter (DJF) and western North America in spring (MAM). Nearly all of the land regions in the northern hemisphere have experienced warmer summers (JJA) and falls (SON).

Figure 9 shows linear trends from 1986–2006 in gridded NDVI averaged over the "growing season" (April through October) and for the month of July. Widespread greening trends are observed, with the exception of browning in the southern boreal forest of North America. Significant greening trends are found in tundra regions, especially in North America.

5   Figure 10a averages the growing season NDVI over the latitude bands, for each year, showing both the growing season average (top panel) and seasonal maximum (bottom panel). The period 1986-2006 showed no significant trend in the 50–60°N band in either growing season or maximum metrics (Fig. 9). In contrast, a significant increasing trend of 0.13% yr^{-1} (Table 2, p=0.01) is found in the >60°N band over this period, driven mostly by trends in tundra regions. Although not included in the trend analysis, growing

10   season NDVI north of 60°N increased abruptly at the end of the record by ~5% from 2009 to 2010. Similarly large changes occurred in 1991–1992 and 1996–1997.

Figure 10b shows the trend in annual peak NDVI, the maximum monthly value for each year regardless of which month it is. This also shows a small but significant increase north of 60°N, 0.12% yr^{-1} (Table 2,p=0.0103) from 1986-2006 and no significant trend in the 50-60°N region. Compared to growing season

15   NDVI, the peak NDVI increase from 2009 to 2010 was less extreme. Plant growth in 2010 was increased in the shoulder seasons in addition to the mid-season peak.

3.6 Controls of temperature and NDVI on CO_2 fluxes

Summer uptake and fall release of CO_2 play a large role in atmospheric CO_2 fluxes and concentration amplitude, so here we look at the correlations of CO_2 fluxes with temperature and NDVI as proxies for

20   primary productivity and soil respiration variability to help assess mechanistic links. We performed lagged correlation analysis on monthly time series by calculating the temporal correlation for either the July net CO_2 fluxes or fall (SON) fluxes and 3 month running means of temperature or NDVI time series with 0 to 60 month (up to 5 year) lags. In this analysis, all data sets were de-trended using a stiff spline to remove long-term trends, thus emphasizing processes controlling interannual variability (IAV).

Figure 11 shows the lagged correlations for the period 1986–2006 of both inversions for the Boreal zone. We found significantly strong positive correlations between July CO_2 flux and April through August temperatures of the same year, but no evidence of correlation with NDVI. The temperature correlation suggests that warmer growing season temperatures increase soil respiration (or wildfires) and result in

30   reduced peak CO_2 uptake (less negative NEE). The fall CO_2 fluxes were also positively correlated with growing season temperatures of the same year (not shown). This is consistent with increased growing season air temperatures stimulating soil respiration through the fall, either through increased carbon pools from enhanced summer productivity or warmer soil temperatures that persist into the fall.

An analysis of the peak July NDVI correlations with lagged air temperatures showed that warmer temperatures in the 14 months prior to the peak NDVI were associated with higher NDVI in the boreal zone (Fig. 12). One possible interpretation of the correlation analyses presented here is that warmer temperatures in the boreal zone lead to increased plant productivity (indicated by positive NDVI and temperature correlation), but that the IAV of the net C balance in July and the fall was dominated by respiration (indicated by positive NEE and temperature correlation and by the lack of an NDVI and NEE correlation).

Lagged correlations for the arctic zone were generally less significant (Fig. S2). July CO_2 fluxes did not show a strong correlation with either temperature or NDVI. Fall CO_2 fluxes were not consistently correlated with temperatures in the same season in either inversion. Peak July NDVI was weakly correlated with May-June temperatures. Overall, we conclude that this northern region may be dominated by other controls, like soil thermal processes that would not show up clearly in the correlation analysis with air temperature and NDVI.

4 Discussion

The results of these two inversion estimates show that the northern high latitude regions of BNA+BA remain nearly constant or slightly increasing sinks of atmospheric CO_2. The Boreal zone, again excluding Europe, absorbed an extra 8–11 Tg C yr^{-1} over the period from 1986 to 2006, resulting in an annual CO_2 sink in 2006 that was 170–230 Tg C larger than in 1986. This trend towards increasing CO_2 uptake appears to continue through 2012 as indicated by the longer Jena s85 inversion. This result contradicts some modeling studies, which point to trend reversals in observed NDVI and modeled net CO_2 fluxes. Hayes et al. (2011) used the TEM ecosystem model to show that increased respiration and fires in this region had weakened the sink strength since 1997. Dynamic global vegetation models have also predicted a trend toward CO_2 release to the atmosphere across much of the northern land region from 1990–2009 (Sitch et al., 2015). In general, Carvalhais et al. (2014) found that models tend to over-predict the transfer of carbon from the soils to the atmosphere and overestimate the sensitivity of heterotrophic respiration to climate, although they didn't include the TEM model used by Hayes et al. (2011). The results of this inversion analysis suggest that respiration is over-predicted in models or that increased primary production not captured by these models is offsetting increases in soil respiration and/or forest fire emissions.

Sensor drift and calibration errors may have resulted in false browning trends in the boreal forest, particularly in the needle-leaf evergreen forests. Recent analyses of NDVI trends in the updated GIMMS3g version find significantly more greening trends than in the previous GIMMSg version observed (Bi et al., 2013; Guay et al., 2014). On a pan-boreal basis, it seems plausible that the CO_2 sink strength has continued to increase despite previous reports of drought stress reducing CO_2 uptake of the boreal region. As a complication, however, any changes in net carbon fluxes in these ecosystems will depend not only on

above ground vegetation changes that can be observed by remote sensing, but also on processes occurring below ground, where most of the carbon is stored (Iversen et al., 2015).

For the Arctic zone, we estimate that July CO_2 uptake increased from 1986 to 2006 by 0.15 to 0.27 g C m^{-2} day^{-1}, depending on the inversion and the trend detection algorithm. This estimate is based on multiplying the regression slopes (Table 2) by the 21-year time frame. In this zone, we found the strongest NDVI greening trends in the tundra regions, covering roughly 25% of the relevant land area. In light of evidence of rapid shrub expansion in these tundra ecosystems (Myers-Smith et al., 2011; Tape et al., 2006) (Elmendorf et al., 2012), a rapid increase in July CO_2 uptake by the tundra ecosystems is plausible.

Most of the previous studies investigating seasonal variability in the northern ecosystem carbon fluxes have relied on observations of atmospheric CO_2 concentrations (Angert et al., 2005; Buermann et al., 2013; Keeling et al., 1996; Piao et al., 2008; e.g. Randerson et al., 1999). The analysis presented here is unique in that it considers variability in atmospheric transport through the inversion model approach. Our results are generally consistent with the finding of Piao et al. (2008) that enhanced CO_2 losses from northern ecosystems in the fall partially cancel the enhanced CO_2 uptake earlier in the growing season, especially in the arctic zone. We also find evidence of uptake enhancement in the summer as well as the spring in both the arctic and boreal zones, consistent with Graven et al. (2013). Increased summer CO_2 uptake cannot be explained by earlier spring leaf-out, but rather points to changes in mid-summer photosynthetic and respiration fluxes themselves.

Our investigation of the controls on interannual variability of the CO_2 fluxes showed increased CO_2 uptake in cooler summers. There are many previous attempts to identify the short-term drivers of the net carbon balance of ecosystems from eddy covariance studies. Several studies have found that warm and dry summers lead to drought stress and reduced net CO_2 uptake in boreal forest ecosystems (Arain et al., 2002; McMillan et al., 2008; Welp et al., 2007). Net CO_2 flux reductions could be the result of decreased primary productivity, increased respiration, or both. Correlations between temperature and annual tree ring growth increments point to a switch from a positive correlation to a negative correlation (reduced growth during warm years) driven by increased drought stress in recent decades (Barber et al., 2000; Beck et al., 2011). Wunch et al. (2013) found that total column CO_2 in the north was relatively higher during years with warm anomalies in the boreal region, suggesting that reduced net CO_2 uptake during warm summers may driven by the temperature dependence of soil respiration. These correlations of interannual variability are contrary to the overall long-term association with warming and greater summer uptake (Keeling et al., 1996). This difference could reflect the importance of structural ecosystem changes due to warming on the long time scale increasing photosynthesis (Graven et al., 2013), but on the short time scale, respiration is the dominant control.

A full explanation of the trends in CO_2 fluxes of the arctic and boreal zones is still lacking, with possible causes including changes in temperature, which were explored here, but also soil moisture, nutrient status,

or fire and insect disturbance. An important unresolved question is how the distribution of deciduous and evergreen plant functional types has changed at the pan-boreal scale over this period. A shift to younger forests, with increasing deciduous fraction, would increase the seasonal flux amplitude (Welp et al., 2006; Zimov, 1999), perhaps with little change in common NDVI metrics.

5   The latitude gradient of changes in land fluxes from the Jena inversion, now including results from Europe, shows that, from the 1985–1989 mean to the 2007–2011 mean, the surface flux amplitudes have increased the most from 40°N to 65°N (Fig. 7a). This is consistent with Graven et al. (2013), who argued that, over the longer period from 1960–2010, the increases in CO_2 flux amplitude were centered mostly on boreal regions. Our analysis of the Jena inversion by latitudinal bands shows that the increases in peak July
10 uptake have been greater than the fall CO_2 releases north of 55°N, but from 40–55°N, fall release out-paced July uptake (Fig. 7b). The results presented here show that the increased seasonal amplitude in atmospheric CO_2 in the high northern latitudes isn't caused by flux trends in the summer or fall only, but rather both contribute (Fung, 2013; Graven et al., 2013). The trend in annual net CO_2 fluxes also includes changes in other months, with namely greater uptake in the spring (not shown in Fig. 7), which contributes
15 to the annual sum. The advantage of this analysis is that it incorporates interannually varying atmospheric transport, so the temporal changes in the surface fluxes should be better resolved. It does not identify whether individual months have a disproportionately larger influence on the atmospheric CO_2 concentration amplitude.

    Our attempt to distinguish changes by ~10° latitude arctic and boreal zones is pushing the limits of what is
20 feasible from atmospheric inversions based on sparse atmospheric CO_2 observations. The limitation is illustrated by the tendency of the two inverse calculations to allocate the increase in fall CO_2 release mostly to different bands and the shift to increasing earlier CO_2 uptake in the Jena model compared to the RIGC model in Figure 3c. Resolving fluxes with monthly resolution is also challenging (Broquet et al., 2013), but the long record examined here, by two independent inversions, gives us reasonable confidence in this
25 aspect.

5   Conclusions

The two atmospheric inversions analyzed in this study show that the annual net CO_2 sink strength in the boreal zone has increased from 1985–2012. However, the annual net CO_2 fluxes in arctic zone showed no trend. In both zones, a trend towards greater CO_2 emissions in the fall has partly canceled the trend toward
30 greater summer uptake, with greater cancelation in the arctic zone. These trends in summer and fall fluxes cause the seasonal amplitude of the fluxes, and consequently the seasonal amplitude of atmospheric CO_2 concentrations, to increase. We also discussed some evidence from NDVI and CO_2 flux interannual correlations suggesting that while warmer summers were correlated with increasing NDVI, relatively cooler summers favor net CO_2 uptake in the boreal region in the short term. Overall, there is evidence from

these atmospheric inversions that increased CO_2 uptake overall is offsetting carbon release in the pockets of browning in the boreal zone. In the arctic zone, shrub expansion and dramatic greening in the tundra has not influenced the net annual CO_2 sink of the region. These atmospheric inversions studied, spanning the period from 1985–2012, show no evidence of weakening year-round sink or growing CO_2 source, as might

5   be expected from an incipient 'carbon bomb'.

Data Availability

The data used this in this analysis is publically available from the individuals authors responsible for creating the products. The Jena CO_2 inversion results are posted to the project website, http://www.bgc-jena.mpg.de/~christian.roedenbeck/download-CO_2/. Run ID s85 version 3.6 was used in this project.

10   Associated files contain the atmospheric monitoring site locations and data used in the inversion and the fossil fuel emissions that were used to solve for the biological land CO_2 fluxes. The RIGC CO_2 inversion results are posted on the Global Carbon Atlas project website, http://www.globalcarbonatlas.org/?q=en/content/atmospheric-inversions. Likewise, associated files contain the atmospheric monitoring site locations and data used in the inversion and the fossil fuel emissions that

15   were used to solve for the biological land CO_2 fluxes. The GIMMS NDVI3g data used is posted on the AVHRR website, https://nex.nasa.gov/nex/projects/1349/. After the final acceptance of this manuscript, the code used in the analysis will be posted on GitHub.

Acknowledgements

This project was supported by NASA under award NNX11AF36G, the U.S. Department of Energy under

20   awards DE-SC0005090 and DE-SC0012167, NSF under award PLR-1304270 and UC Multiple Campus Award Number UCSCMCA-14-015. Any opinions, findings, and conclusions or recommendations expressed in this material are those of the authors and do not necessarily reflect the views of the NASA, NSF, DOE, or UC.

References

ACIA: Impacts of a warming Arctic: Arctic Climate Impact Assessment, Cambridge University Press. 2004.

5 Angert, A., Biraud, S., Bonfils, C., Henning, C. C., Buermann, W., Pinzon, J., Tucker, C. J. and Fung, I.: Drier summers cancel out the CO_2 uptake enhancement induced by warmer springs, Proc. Natl. Acad. Sci. U.S.A., 102(31), 10823–10827, doi:10.1073/pnas.0501647102, 2005.

Arain, M. A., Black, T. A., Barr, A. G., Jarvis, P. G., Massheder, J. M., Verseghy, D. L. and Nesic, Z.: Effects of seasonal and interannual climate variability on net ecosystem productivity of boreal deciduous
10 and conifer forests, Canadian Journal of Forest Research, 32(5), 878–891, doi:10.1139/x01-228, 2002.

Baker, D. F., Law, R. M., Gurney, K. R., Rayner, P., Peylin, P., Denning, A. S., Bousquet, P., Bruhwiler, L., Chen, Y.-H., Ciais, P., Fung, I. Y., Heimann, M., John, J., Maki, T., Maksyutov, S., Masarie, K., Prather, M., Pak, B., Taguchi, S. and Zhu, Z.: TransCom 3 inversion intercomparison: Impact of transport model errors on the interannual variability of regional CO_2 fluxes, 1988–2003, Global Biogeochemical
15 Cycles, 20(1), GB1002, doi:10.1029/2004GB002439, 2006.

Barber, V. A., Juday, G. P. and Finney, B. P.: Reduced growth of Alaskan white spruce in the twentieth century from temperature-induced drought stress, Nature, 405(6787), 668–673, 2000.

Beck, P. S. A., Juday, G. P., Alix, C., Barber, V. A., Winslow, S. E., Sousa, E. E., Heiser, P., Herriges, J. D. and Goetz, S. J.: Changes in forest productivity across Alaska consistent with biome shift, Ecology
20 Letters, 14(4), 373–379, doi:10.1111/j.1461-0248.2011.01598.x, 2011.

Bekryaev, R. V., Polyakov, I. V. and Alexeev, V. A.: Role of polar amplification in long-term surface air temperature variations and modern Arctic warming, J. Climate, 23(14), 3888–3906, doi:10.1175/2010JCLI3297.1, 2010.

Bi, J., Xu, L., Samanta, A., Zhu, Z. and Myneni, R.: Divergent Arctic-boreal vegetation changes between
25 North America and Eurasia over the past 30 years, Remote Sensing, 5(5), 2093–2112, doi:10.3390/rs5052093, 2013.

Boden, T. A., Marland, G. and Andres, R. J.: Global, regional, and national fossil-fuel CO_2 emissions, Carbon Dioxide Information Analysis Center (CDIAC), Oak Ridge National Laboratry, U.S. Department of Energy, Oak Ridge, Tenn., U.S.A., 2009.

30 Bradshaw, C. J. A. and Warkentin, I. G.: Global estimates of boreal forest carbon stocks and flux, Global and Planetary Change, 128, 24–30, doi:10.1016/j.gloplacha.2015.02.004, 2015.

Broquet, G., Chevallier, F., Breon, F. M., Kadygrov, N., Alemanno, M., Apadula, F., Hammer, S., Haszpra, L., Meinhardt, F., Morguí, J. A., Necki, J., Piacentino, S., Ramonet, M., Schmidt, M., Thompson, R. L., Vermeulen, A. T., Yver, C. and Ciais, P.: Regional inversion of CO_2 ecosystem fluxes from atmospheric
35 measurements: reliability of the uncertainty estimates, Atmos. Chem. Phys., 13(17), 9039–9056, doi:10.5194/acp-13-9039-2013, 2013.

Buermann, W., Bikash, P. R., Jung, M., Burn, D. H. and Reichstein, M.: Earlier springs decrease peak summer productivity in North American boreal forests, Environmental Research Letters, 8(2), 024027, doi:10.1088/1748-9326/8/2/024027, 2013.

40 Carvalhais, N., Forkel, M., Khomik, M., Bellarby, J., Jung, M., Migliavacca, M., Mu, M., Saatchi, S., Santoro, M., Thurner, M., Weber, U., Ahrens, B., Beer, C., Cescatti, A., Randerson, J. T. and Reichstein, M.: Global covariation of carbon turnover times withclimate in terrestrial ecosystems, Nature, 514(7521), 213–217, doi:10.1038/nature13731, 2014.

Cess, R. D., Potter, G. L., Zhang, M. H., Blanchet, J. P., Chalita, S., Colman, R., Dazlich, D. A., Genio, A. D., Dymnikov, V., Galin, V., Jerrett, D., Keup, E., Lacis, A. A., LE Treut, H., Liang, X. Z., Mahfouf, J. F., McAvaney, B. J., Meleshko, V. P., Mitchell, J. F., Morcrette, J. J., Norris, P. M., Randall, D. A., Rikus, L., Roeckner, E., Royer, J. F., Schlese, U., Sheinin, D. A., Slingo, J. M., Sokolov, A. S., Taylor, K. E.,
5   Washington, W. M., Wetherald, R. T. and Yagai, I.: Interpretation of snow-climate feedback as produced by 17 general circulation models, Science, 253(5022), 888–892, doi:10.1126/science.253.5022.888, 1991.

Chapin, F. S.: Role of Land-Surface Changes in Arctic Summer Warming, Science, 310(5748), 657–660, doi:10.1126/science.1117368, 2005.

Comiso, J. C., Parkinson, C. L., Gersten, R. and Stock, L.: Accelerated decline in the Arctic sea ice cover,
10   Geophys. Res. Lett., 35(1), L01703, doi:10.1029/2007GL031972, 2008.

EDGAR: Emission Database for Global Atmospheric Research (EDGAR), release version 4.2, [online] Available from: http://edgar.jrc.ec.europa.eu/, 2011.

Elmendorf, S. C., Henry, G. H. R., Hollister, R. D., Björk, R. G., Boulanger-Lapointe, N., Cooper, E. J., Cornelissen, J. H. C., Day, T. A., Dorrepaal, E., Elumeeva, T. G., Gill, M., Gould, W. A., Harte, J., Hik, D.
15   S., Hofgaard, A., Johnson, D. R., Johnstone, J. F., Jónsdóttir, I. S., Jorgenson, J. C., Klanderud, K., Klein, J. A., Koh, S., Kudo, G., Lara, M., Lévesque, E., Magnússon, B., May, J. L., Mercado-Dı az, J. A., Michelsen, A., Molau, U., Myers-Smith, I. H., Oberbauer, S. F., Onipchenko, V. G., Rixen, C., Martin Schmidt, N., Shaver, G. R., Spasojevic, M. J., Þórhallsdóttir, Þ. E., Tolvanen, A., Troxler, T., Tweedie, C. E., Villareal, S., Wahren, C.-H., Walker, X., Webber, P. J., Welker, J. M. and Wipf, S.: Plot-scale evidence
20   of tundra vegetation change and links to recent summer warming, Nature Climate Change, 2(6), 453–457, doi:10.1038/nclimate1465, 2012.

Enting, I. G.: Inverse problems in atmospheric constituent transport, Cambridge University Press. 2002.

Forkel, M., Carvalhais, N., Verbesselt, J., Mahecha, M., Neigh, C. and Reichstein, M.: Trend change detection in NDVI time series: effects of inter-annual variability and methodology, Remote Sensing, 5(5),
25   2113–2144, doi:10.3390/rs5052113, 2013.

Francis, J. A., Chan, W., Leathers, D. J., Miller, J. R. and Veron, D. E.: Winter Northern Hemisphere weather patterns remember summer Arctic sea-ice extent, Geophys. Res. Lett., 36(7), doi:10.1029/2009GL037274, 2009.

Fung, I.: Atmospheric science. A hyperventilating biosphere, Science, 341(6150), 1075–1076,
30   doi:10.1126/science.1242004, 2013.

Giglio, L., Randerson, J. T. and Van Der Werf, G. R.: Analysis of daily, monthly, and annual burned area using the fourth-generation global fire emissions database (GFED4), J. Geophys. Res. Biogeosci., 118(1), 317–328, doi:10.1002/jgrg.20042, 2013.

Goetz, S. J., Bunn, A. G., Fiske, G. J. and Houghton, R. A.: Satellite-observed photosynthetic trends across
35   boreal North America associated with climate and fire disturbance, Proc. Natl. Acad. Sci. U.S.A., 102(38), 13521–13525, 2005.

Goetz, S. J., Mack, M. C., Gurney, K. R., Randerson, J. T. and Houghton, R. A.: Ecosystem responses to recent climate change and fire disturbance at northern high latitudes: observations and model results contrasting northern Eurasia and North America, Environmental Research Letters, 2(4), 045031,
40   doi:10.1088/1748-9326/2/4/045031, 2007.

Graven, H. D., Keeling, R. F., Piper, S. C., Patra, P. K., Stephens, B. B., Wofsy, S. C., Welp, L. R., Sweeney, C., Tans, P. P., Kelley, J. J., Daube, B. C., Kort, E. A., Santoni, G. W. and Bent, J. D.: Enhanced seasonal exchange of CO_2 by northern ecosystems since 1960, Science, 341(6150), 1085–1089,

doi:10.1126/science.1239207, 2013.

Guay, K. C., Beck, P. S. A., Berner, L. T., Goetz, S. J., Baccini, A. and Buermann, W.: Vegetation productivity patterns at high northern latitudes: a multi-sensor satellite data assessment, Global Change Biol, 20(10), 3147–3158, doi:10.1111/gcb.12647, 2014.

5   Gurney, K. R., Law, R. M., Denning, A. S. and Rayner, P. J.: TransCom 3 CO_2 inversion intercomparison: 1. Annual mean control results and sensitivity to transport and prior flux information, Tellus B, 2003.

Hansen, J., Ruedy, R. and Glascoe, J.: GISS analysis of surface temperature change, J. Geophys. Res., 104(D24), 30–997–31–022, 1999.

Hayes, D. J., Mcguire, A. D., Kicklighter, D. W., Gurney, K. R., Burnside, T. J. and Melillo, J. M.: Is the
10   northern high-latitude land-based CO_2 sink weakening? Global Biogeochemical Cycles, 25(3), doi:10.1029/2010GB003813, 2011.

Higuchi, K.: Quasi-decadal variation of the atmospheric CO 2seasonal cycle due to atmospheric circulation changes: 1979–1998, Geophys. Res. Lett., 29(8), 1173, doi:10.1029/2001GL013751, 2002.

Hinzman, L. D., Bettez, N. D., Bolton, W. R., Chapin, F. S., Dyurgerov, M. B., Fastie, C. L., Griffith, B.,
15   Hollister, R. D., Hope, A., Huntington, H. P., Jensen, A. M., Jia, G. J., Jorgenson, T., Kane, D. L., Klein, D. R., Kofinas, G., Lynch, A. H., Lloyd, A. H., McGuire, A. D., Nelson, F. E., Oechel, W. C., Osterkamp, T. E., Racine, C. H., Romanovsky, V. E., Stone, R. S., Stow, D. A., Sturm, M., Tweedie, C. E., Vourlitis, G. L., Walker, M. D., Walker, D. A., Webber, P. J., Welker, J. M., Winker, K. S. and Yoshikawa, K.: Evidence and Implications of Recent Climate Change in Northern Alaska and Other Arctic Regions,
20   Climatic Change, 72(3), 251–298, doi:10.1007/s10584-005-5352-2, 2005.

Hogg, E. H. T., Brandt, J. P. and Michaelian, M.: Impacts of a regional drought on the productivity, dieback, and biomass of western Canadian aspen forests, Canadian Journal of Forest Research, 38(6), 1373–1384, doi:10.1139/X08-001, 2008.

Holland, E. A., Braswell, B. H., Lamarque, J.-F., Townsend, A., Sulzman, J., Müller, J.-F., Dentener, F.,
25   Brasseur, G., Levy, H., II and Penner, J. E.: Variations in the predicted spatial distribution of atmospheric nitrogen deposition and their impact on carbon uptake by terrestrial ecosystems, J. Geophys. Res., 102(D13), 15–849–15–866, 1997.

Iversen, C. M., Sloan, V. L., Sullivan, P. F., Euskirchen, E. S., McGuire, A. D., Norby, R. J., Walker, A. P., Warren, J. M. and Wullschleger, S. D.: The unseen iceberg: plant roots in arctic tundra, New Phytol,
30   205(1), 34–58, doi:10.1111/nph.13003, 2015.

Keeling, C. D., Chin, J. and Whorf, T. P.: Increased activity of northern vegetation inferred from atmospheric CO_2 measurements, Nature, 382(6587), 146–149, 1996.

Kimball, J. S., Zhao, M., Mcguire, A. D., Heinsch, F. A., Clein, J., Calef, M., Jolly, W. M., Kang, S., Euskirchen, S. E., McDonald, K. C. and Running, S. W.: Recent climate-driven increases in vegetation
35   productivity for the western Arctic: Evidence of an acceleration of the northern terrestrial carbon cycle, Earth Interact, 11, 1–30, 2007.

Kurz, W. A., Dymond, C. C., Stinson, G., Rampley, G. J., Neilson, E. T., Carroll, A. L., Ebata, T. and Safranyik, L.: Mountain pine beetle and forest carbon feedback to climate change, Nature, 452(7190), 987– 990, doi:10.1038/nature06777, 2008.

40   Lloyd, A. H., Wilson, A. E., Fastie, C. L. and Landis, R. M.: Population dynamics of black spruce and white spruce near the arctic tree line in the southern Brooks Range, Alaska, Canadian Journal of Forest Research, 35(9), 2073–2081, doi:10.1139/x05-119, 2005.

Lloyd, J. and Farquhar, G. D.: The CO_2 dependence of photosynthesis, plant growth responses to elevated atmospheric CO_2 concentrations and their interaction with soil nutrient status. I. General principles and forest ecosystems, Functional Ecology, 10(1), 4–32, 1996.

5   Ma, Z., Peng, C., Zhu, Q., Chen, H. and Yu, G.: Regional drought-induced reduction in the biomass carbon sink of Canada's boreal forests, vol. 109, pp. 2423–2427. 2012.

McDonald, K. C., Kimball, J. S., Njoku, E., Zimmermann, R. and Zhao, M.: Variability in springtime thaw in the terrestrial high latitudes: monitoring a major control on the biospheric assimilation of atmospheric CO_2 with spaceborne microwave remote sensing, Earth Interact, 8, 1–22, 2004.

10   McGuire, A. D., Anderson, L. G., Christensen, T. R., Dallimore, S., Guo, L., Hayes, D. J., Heimann, M., Lorenson, T. D., Macdonald, R. W. and Roulet, N.: Sensitivity of the carbon cycle in the Arctic to climate change, Ecological Monographs, 79(4), 523–555, 2009.

McGuire, A. D., Hayes, D. J., Kicklighter, D. W., Manizza, M., Zhuang, Q., Chen, M., Follows, M. J., Gurney, K. R., Mcclelland, J. W., Melillo, J. M., Peterson, B. J. and Prinn, R. G.: An analysis of the carbon balance of the Arctic Basin from 1997 to 2006, Tellus B, 62(5), 455–474, doi:10.1111/j.1600-15   0889.2010.00497.x, 2010.

McGuire, A. D., Sitch, S., Clein, J. S., Dargaville, R., Esser, G., Foley, J., Heimann, M., Joos, F., Kaplan, J., Kicklighter, D. W., Meier, R. A., Melillo, J. M., Moore, B., III, Prentice, I. C., Ramankutty, N., Reichenau, T., Schloss, A., Tian, H., Williams, L. J. and Wittenberg, U.: Carbon balance of the terrestrial biosphere in the twentieth century: Analyses of CO_2, climate and land use effects with four process-based 20   ecosystem models, Global Biogeochemical Cycles, 15, 183–206, 2001.

McMillan, A. M. S., Winston, G. C. and Goulden, M. L.: Age-dependent response of boreal forest to temperature and rainfall variability, Global Change Biol, 14(8), 1904–1916, doi:10.1111/j.1365-2486.2008.01614.x, 2008.

Michaelian, M., Hogg, E. H., Hall, A. E. and Arsenault, E.: Massive mortality of aspen following severe 25   drought along the southern edge of the Canadian boreal forest, Global Change Biol, 17(6), 2084–2094, doi:10.1111/j.1365-2486.2010.02357.x, 2010.

Mikaloff Fletcher, S. E., Gruber, N., Jacobson, A. R., Doney, S. C., Dutkiewicz, S., Gerber, M., Follows, M., Joos, F., Lindsay, K., Menemenlis, D., Mouchet, A., Müller, S. A. and Sarmiento, J. L.: Inverse estimates of anthropogenic CO_2 uptake, transport, and storage by the ocean, Global Biogeochemical 30   Cycles, 20(2), n/a–n/a, doi:10.1029/2005GB002530, 2006.

Myers-Smith, I. H., Forbes, B. C., Wilmking, M., Hallinger, M., Lantz, T., Blok, D., Tape, K. D., Macias-Fauria, M., Sass-Klaassen, U., Lévesque, E., Boudreau, S., Ropars, P., Hermanutz, L., Trant, A., Collier, L. S., Weijers, S., Rozema, J., Rayback, S. A., Schmidt, N. M., Schaepman-Strub, G., Wipf, S., Rixen, C., Ménard, C. B., Venn, S., Goetz, S., Andreu-Hayles, L., Elmendorf, S., Ravolainen, V., Welker, J., Grogan, 35   P., Epstein, H. E. and Hik, D. S.: Shrub expansion in tundra ecosystems: dynamics, impacts and research priorities, Environmental Research Letters, 6(4), 045509, doi:10.1088/1748-9326/6/4/045509, 2011.

Myneni, R. B., Keeling, C. D., Tucker, C. J., Asrar, G. and Nemani, R. R.: Increased plant growth in the northern high latitudes from 1981 to 1991, Nature, 386(6626), 698–702, 1997.

Oliver, J. G. and Berdowski, J. J. M.: Global emissions sources and sinks, in The Climate System, edited by 40   J. J. M. Berdowski, R. Guicherit, B. J. Heiji, and A. A. Balkema, Swets and Zeitlinger Publishers, Lisse, The Netherlands. 2001.

Patra, P., Maksyutov, S., Ishizawa, M., Nakazawa, T., Takahashi, T. and Ukita, J.: Interannual and decadal changes in the sea-air CO_2 flux from atmospheric CO_2 inverse modeling, Global Biogeochemical Cycles,

19, GB4013, doi:10.1029/2004GB002257, 2005.

Pearson, R. G., Phillips, S. J., Loranty, M. M., Beck, P. S. A., Damoulas, T., Knight, S. J. and Goetz, S. J.: Shifts in Arctic vegetation and associated feedbacks under climate change, Nature Climate Change, 3(4), 1–5, doi:10.1038/nclimate1858, 2013.

5 Peng, C., Ma, Z., Lei, X., Zhu, Q., Chen, H., Wang, W., Liu, S., Li, W., Fang, X. and Zhou, X.: A drought-induced pervasive increase in tree mortality across Canada's boreal forests, Nature Climate Change, 1(9), 467–471, doi:10.1038/nclimate1293, 2011.

Piao, S., Ciais, P., Friedlingstein, P., Peylin, P., Reichstein, M., Luyssaert, S., Margolis, H., Fang, J., Barr, A., Chen, A., Grelle, A., Hollinger, D. Y., Laurila, T., Lindroth, A., richardson, A. D. and Vesala, T.: Net 10 carbon dioxide losses of northern ecosystems in response to autumn warming, Nature, 451(7174), 49–52, doi:10.1038/nature06444, 2008.

Pinzon, J. and Tucker, C.: A non-stationary 1981–2012 AVHRR NDVI3g time series, Remote Sensing, 6(8), 6929–6960, doi:10.3390/rs6086929, 2014.

Qu, X. and Hall, A.: What Controls the Strength of Snow-Albedo Feedback? J. Climate, 20(15), 3971– 15 3981, doi:10.1175/JCLI4186.1, 2007.

Randerson, J. T., Field, C. B., Fung, I. Y. and Tans, P. P.: Increases in early season ecosystem uptake explain recent changes in the seasonal cycle of atmospheric CO_2 at high northern latitudes, Geophys. Res. Lett., 26(17), 2765–2768, 1999.

Rayner, P. J., Enting, I. G., Francey, R. J. and Langenfelds, R.: Reconstructing the recent carbon cycle from 20 atmospheric CO_2, $\delta^{13}C$ and O_2/N_2 observations, Tellus B, 51B, 213–232, 1999.

Rodenbeck, C.: Estimating CO_2 sources and sinks from atmospheric mixing ratio measurements using a global inversion of atmospheric transport, Max Planck Institute for Biogeochemistry, Jena. 2005.

Romanovsky, V. E., Smith, S. L. and Christiansen, H. H.: Permafrost thermal state in the polar Northern Hemisphere during the international polar year 2007-2009: a synthesis, Permafrost Periglac. Process., 25 21(2), 106–116, doi:10.1002/ppp.689, 2010.

Schultz, M. G., Heil, A., Hoelzemann, J. J., Spessa, A., Thonicke, K., Goldammer, J. G., Held, A. C., Pereira, J. M. C. and van het Bolscher, M.: Global wildland fire emissions from 1960 to 2000, Global Biogeochemical Cycles, 22, GB2002, doi:10.1029/2007GB003031, 2008.

Schuur, E., Bockheim, J. and Canadell, J. G.: Vulnerability of permafrost carbon to climate change: 30 Implications for the global carbon cycle, BioScience, 58(8), 701–714, 2008.

Serreze, M. C. and Barry, R. G.: Processes and impacts of Arctic amplification: A research synthesis, Global and Planetary Change, 77(1-2), 85–96, doi:10.1016/j.gloplacha.2011.03.004, 2011.

Serreze, M. C., Walsh, J. E., Chapin, F. S., III, Osterkamp, T., Dyurgerov, M., Romanovsky, V., Oechel, W. C., Morison, J., Zhang, T. and Barry, R. G.: Observational evidence of recent change in the northern 35 high-latitude environment, Climatic Change, 46(1-2), 159–207, 2000.

Sitch, S., Friedlingstein, P., Gruber, N., Jones, S. D., Murray-Tortarolo, G., Ahlström, A., Doney, S. C., Graven, H., Heinze, C., Huntingford, C., Levis, S., Levy, P. E., Lomas, M., Poulter, B., Viovy, N., Zaehle, S., Zeng, N., Arneth, A., Bonan, G., Bopp, L., Canadell, J. G., Chevallier, F., Ciais, P., Ellis, R., Gloor, M., Peylin, P., Piao, S. L., Le Quere, C., Smith, B., Zhu, Z. and Myneni, R.: Recent trends and drivers of 40 regional sources and sinks of carbon dioxide, Biogeosciences, 12(3), 653–679, doi:10.5194/bg-12-653-2015-supplement, 2015.

Smith, N. V.: Trends in high northern latitude soil freeze and thaw cycles from 1988 to 2002, J. Geophys. Res., 109(D12), D12101, doi:10.1029/2003JD004472, 2004.

Sturm, M.: Changing snow and shrub conditions affect albedo with global implications, J. Geophys. Res., 110(G1), G01004, doi:10.1029/2005JG000013, 2005.

5   Takahashi, T., Sutherland, S. C. and Sweeney, C.: Global sea–air CO_2 flux based on climatological surface ocean pCO_2, and seasonal biological and temperature effects, Deep Sea Research …, 49, 1601–1622, 2002.

Tape, K. D., Sturm, M. and Racine, C. H.: The evidence for shrub expansion in Northern Alaska and the Pan-Arctic, Global Change Biol, 12(4), 686–702, doi:10.1111/j.1365-2486.2006.01128.x, 2006.

van der Werf, G. R., Randerson, J. T., Giglio, L., Collatz, G. J., Kasibhatla, P. S. and Arellano, A. F., Jr.:
10   Interannual variability in global biomass burning emissions from 1997 to 2004, Atmos. Chem. Phys., 6(11), 3423–3441, doi:10.5194/acp-6-3423-2006, 2006.

Verbyla, D.: The greening and browning of Alaska based on 1982–2003 satellite data, Global Ecol Biogeography, 17(4), 547–555, doi:10.1111/j.1466-8238.2008.00396.x, 2008.

Verbyla, D.: Browning boreal forests of western North America, Environmental Research Letters, 6(4),
15   041003, doi:10.1088/1748-9326/6/4/041003, 2011.

Walther, G. R.: Community and ecosystem responses to recent climate change, Philosophical Transactions of the Royal Society B: Biological Sciences, 365(1549), 2019–2024, doi:10.1016/j.tree.2009.06.008, 2010.

Welp, L. R., Randerson, J. T. and Liu, H. P.: Seasonal exchange of CO_2 and $\delta^{18}O$-CO_2 varies with postfire succession in boreal forest ecosystems, J. Geophys. Res., 111(G3), G03007, doi:10.1029/2005JG000126,
20   2006.

Welp, L. R., Randerson, J. T. and Liu, H. P.: The sensitivity of carbon fluxes to spring warming and summer drought depends on plant functional type in boreal forest ecosystems, Agricultural and Forest Meteorology, 147(3), 172–185, doi:10.1016/j.agrformet.2007.07.010, 2007.

Wunch, D., Wennberg, P. O., Messerschmidt, J., Parazoo, N. C., Toon, G. C., Deutscher, N. M., Keppel-
25   Aleks, G., Roehl, C. M., Randerson, J. T., Warneke, T. and Notholt, J.: The covariation of Northern Hemisphere summertime CO_2 with surface temperature in boreal regions, Atmos. Chem. Phys., 13(18), 9447–9459, doi:10.5194/acp-13-9447-2013, 2013.

Xu, L., Myneni, R. B., Chapin, F. S., III, Callaghan, T. V., Pinzon, J. E., Tucker, C. J., Zhu, Z., Bi, J., Ciais, P., Tømmervik, H., Euskirchen, E. S., Forbes, B. C., Piao, S. L., Anderson, B. T., Ganguly, S., Nemani, R.
30   R., Goetz, S. J., Beck, P. S. A., Bunn, A. G., Cao, C. and Stroeve, J. C.: Temperature and vegetation seasonality diminishment over northern lands, Nature Climate Change, 3(5), 1–6, doi:10.1038/nclimate1836, 2013.

Zhang, K., Kimball, J. S., Hogg, E., Zhao, M., Oechel, W. C., Cassano, J. J. and Running, S. W.: Satellite-based model detection of recent climate-driven changes in northern high-latitude vegetation productivity, J.
35   Geophys. Res., 113(G3), G03–033, 2008.

Zhang, X., Gurney, K. R., Peylin, P., Chevallier, F., Law, R. M., Patra, P. K., Rayner, P., Röedenbeck, C. and Krol, M.: On the variation of regional CO_2 exchange over temperate and boreal North America, Global Biogeochemical Cycles, 27(4), 991–1000, doi:10.1002/gbc.20091, 2013.

Zhou, L., Tucker, C. J., Kaufmann, R. K., Slayback, D., Shabanov, N. V. and Myneni, R. B.: Variations in
40   northern vegetation activity inferred from satellite data of vegetation index during 1981 to 1999, J. Geophys. Res., 106(D17), 20069, doi:10.1029/2000JD000115, 2001.

Zimov, S. A.: Contribution of disturbance to increasing seasonal amplitude of atmospheric CO_2, Science, 284(5422), 1973–1976, doi:10.1126/science.284.5422.1973, 1999.

Table 1. CO$_2$ observation stations included in each inversion model.

Station	Lat	Years	Coverage	RIGC	Jena	Lab
ALT	82.4	1985- 2012	95%	X	X	SIO/NOAA
BRW	71.3	1985 - 2012	100%	X	X	SIO/NOAA
STM	66.0	1985 - 2009	100%	X	X	NOAA
CBA	55.2	1985 - 2012	84%	X	X	NOAA
SHM	52.7	1985 - 2012	88%	X	X	NOAA
SCH	48.0	1985 - 2001	89%	X		UBA
CMN	44.1	1985 - 2012	100%	X	X	NOAA
NWR	40.0	1985 - 2012	100%	X	X	NOAA
RYO	39.0	1987 - 2012	90%	X		NOAA
LJO	32.9	1985 - 2012			X	SIO
BME	32.3	1989 - 2010	81%	X		NOAA
BMW	32.2	1989 - 2012	77%	X		NOAA
MID	28.2	1985 -2012	97%	X		NOAA
KEY	25.6	1985- 2012	95%	X	X	NOAA
MLO	19.5	1985 - 2012	100%	X	X	SIO/NOAA
KUM	19.5	1985 - 2012	100%	X	X	SIO/NOAA
GMI	13.4	1985 - 2012	97%	X		NOAA
RPB	13.1	1987 - 2012	84%	X		NOAA
CHR	1.7	1985 - 2012			X	SIO
SEY	-4.6	1985 - 2012	87%	X		NOAA
ASC	-7.9	1985 - 2012	98%	X	X	NOAA
SMO	-14.2	1985 - 2012	100%	X	X	NOAA
AMS	-37.9	1985 - 1990	89%	X		NOAA
KER	-29.0	1985 - 2012			X	SIO
CGO	-40.6	1985 - 2012	99%	X	X	NOAA
BHD	-41.4	1999 - 2012	71%	X	X	NOAA
PSA	-64.9	1985 - 2012	94%	X	X	NOAA
SYO	-69.0	1986 - 2012	78%	X		NOAA
SPO	-89.9	1985- 2012	97%	X	X	SIO/NOAA

Coverage refers to percent coverage of observation data from 1985 - 2006 used in the RIGC inversion.
Most station records start before 1985 and continue beyond 2012 but that data was not used in this analysis.
5   Lab stations names and data links as following:
NOAA: NOAA ESRL/CMDL, http://www.esrl.noaa.gov/gmd/ccgg/globalview/co2/co2_observations.html
SIO: Scripps Institution of Oceanography, http://cdiac.ornl.gov/trends/co2/sio-keel-flask/
UBA: Umweltbundesamt and University of Heidelberg, Germany, http://cdiac.ornl.gov/trends/co2/uba/uba-
   sc.html

Table 2. Trend and significance statistics for time series of interest, from 1986 through 2006. 'Trend' is the slope from linear least squares (LSQ) and Mann-Kendall (M-K) sen slope, likewise, 'Sig (p-value)' is the p-value from LSQ and M-K tests. Arctic zone and boreal zone are for BNA+BA, EU = Europe, NO = northern ocean. Italic values indicate 90% significance level.

1986-2006				Trend		Sig (p-value)	
Time series	units	zone	inversion	LSQ	M-K	LSQ	M-K
CO_2 flux annual sum	Pg C yr^{-1}	arctic	RIGC	0.0350	0.0051	0.5719	0.2389
		arctic	JENA	-0.0028	-0.0021	0.3550	0.6077
		boreal	*RIGC*	*-0.0110*	*-0.0101*	*0.0724*	*0.0967*
		boreal	JENA	-0.0081	-0.0076	0.1438	0.1941
		EU	RIGC	0.0007	-0.0027	0.9295	0.7398
		EU	JENA	-0.0052	0.0020	0.5092	0.8326
		NO	*RIGC*	*-0.0032*	*-0.0037*	*0.0308*	*0.0320*
		NO	*JENA*	*-0.0014*	*-0.0015*	*0.0005*	*0.0060*
CO_2 flux amplitude	% yr^{-1}	*arctic*	*RIGC*	*0.93*	*0.85*	*0.0019*	*0.0201*
		arctic	*JENA*	*1.04*	*0.97*	*0.0002*	*0.0004*
		boreal	RIGC	0.15	0.22	0.3241	0.2639
		boreal	*JENA*	*0.44*	*0.39*	*0.0328*	*0.0372*
		EU	*RIGC*	*0.62*	*0.55*	*0.0769*	*0.1390*
		EU	JENA	0.18	0.16	0.2723	0.3812
		NO	*RIGC*	*-2.35*	*-2.20*	*0.0192*	*0.0372*
		NO	JENA	0.63	0.65	0.2894	0.2639
CO_2 flux July	g C m^{-2} day^{-1} yr^{-1}	*arctic*	*RIGC*	*-0.0128*	*-0.0120*	*0.0167*	*0.0655*
		arctic	*JENA*	*-0.0072*	*-0.0082*	*0.0004*	*0.0028*
		boreal	RIGC	-0.0058	-0.0034	0.1712	0.3492
		boreal	*JENA*	*-0.0097*	*-0.0085*	*0.0615*	*0.0571*
Fossil fuel emissions	Pg C yr^{-1}	*arctic*	*RIGC*	*-0.0206*	*-0.0011*	*0.0024*	*0.0320*
		arctic	JENA	-0.0159	0.0001	0.9664	0.9759
		EU	*RIGC*	*-0.0013*	*-0.0195*	*<0.0001*	*0.0002*
		EU	*JENA*	*-0.0000*	*-0.0135*	*<0.0001*	*0.0086*
NDVI growing season	% yr^{-1}	*arctic*		*0.1500*	*0.1300*	*0.0112*	*0.0103*
		boreal		0.0587	0.0532	0.3170	0.4503
NDVI peak	% yr^{-1}	*arctic*		*0.1200*	*0.1200*	*0.0109*	*0.0103*
		boreal		0.0030	-0.0043	0.9419	0.9759

Time series	units	zone		LSQ	M-K	LSQ	M-K
Temperature, spring	deg C yr^{-1}	arctic		-0.0124	0.0439	0.8592	0.7858
		boreal		0.0063	0.0192	0.8961	0.6506
Temperature, summer	deg C yr^{-1}	*arctic*		*0.0848*	*0.0915*	*0.0011*	*0.0041*
		boreal		*0.0491*	*0.0527*	*0.0043*	*0.0072*
Temperature, fall	deg C yr^{-1}	*arctic*		*0.0500*	*0.0377*	*0.1559*	*0.0655*
		boreal		*0.0551*	*0.0503*	*0.0080*	*0.0072*
Temperature, winter	deg C yr^{-1}	arctic		-0.0159	-0.0096	0.6961	0.6077
		boreal		-0.0041	0.0122	0.9172	0.8326

Table 3: Same as Table 2, but for the period from 1985 through 2012.

1985-2012				Trend		Sig (p-value)	
Time series	**units**	**zone**	**inversion**	**LSQ**	**M-K**	**LSQ**	**M-K**
CO_2 flux net annual	Pg C yr^{-1}	*arctic*	*JENA*	*-0.0040*	*-0.0038*	*0.0411*	*0.0722*
		boreal	*JENA*	*-0.0072*	*-0.0078*	*0.0655*	*0.1095*
		EU	JENA	-0.0032	0.0005	0.5155	0.9842
		NO	JENA	-0.0010	-0.0010	0.0001	0.0037
CO_2 flux amplitude	% yr^{-1}	*arctic*	*JENA*	*0.81*	*0.85*	*<0.0001*	*0.0001*
		boreal	*JENA*	*0.35*	*0.31*	*0.0094*	*0.0187*
		EU	JENA	<0.01	<0.01	0.4365	0.4179
		NO	JENA	<0.01	<0.01	0.4299	0.3740
CO_2 flux July	g C m^{-2} day^{-1} yr^{-1}	*arctic*	*JENA*	*-0.0068*	*-0.0072*	*<0.0001*	*0.0001*
		boreal	*JENA*	*-0.0083*	*-0.0084*	*0.0345*	*0.0380*

Figure captions

Figure 1: The major land and ocean basis regions used in the RIGC inversion based on the TransCom3 regions. The Jena inversion was done on a ~4x5 degree grid and aggregated to these regions. The northernmost land regions are shown in color. The two zones that we discuss in this analysis cover Boreal North America and Boreal Asia and are marked in shades of blue, with the arctic zone (>60°N) in light blue and the boreal zone (50°N to 60°N) in dark blue. The European basis region, in red, is not divided at 60°N in the RIGC inversion and therefore is not included in this analysis. Stippling indicates the boreal forest biome based on the GLDAS UMD modified IGBP land classification scheme (http://ldas.gsfc.nasa.gov/gldas/GLDASvegetation.php). The tundra biome is north of the stippling.

Figure 2: Annual CO_2 fluxes normalized by subtracting the 1986–2006 mean value for (a) arctic zone (>60°N) and (b) boreal zone (50°N to 60°N). Black shows the RIGC inversion results. Grey shows the Jena s85 inversion results. Dashed lines are linear trends from 1986 to 2006. Negative values represent uptake of CO_2 by the land biosphere, i.e. out of the atmosphere (Table 2).

Figure 3: Mean monthly CO_2 fluxes for (a) arctic zone (>60°N) and (b) boreal zone (50°N to 60°N). Black circles are the 1986–2006 means of the RIGC inversion. Grey squares are the Jena s85 inversion over that same period. Magenta is the Jena inversion average over a longer time period (1985–2012). Differences are likely due to differences in atmospheric transport, including vertical mixing, between the models. Linear monthly trends of (c) arctic zone and (b) boreal zone for the same inversions and time periods as in (a) and (b) (Table 2).

Figure 4: CO_2 flux amplitude for each year calculated as the maximum monthly flux (positive = CO_2 release to the atmosphere) minus the minimum monthly flux (negative = CO_2 uptake by the biosphere) for (a) arctic zone and (b) boreal zone. Black shows the RIGC inversion, grey shows the Jena s85 inversion. Dashed lines show the linear trends from 1986–2006, the common period between the inversions.

Figure 5: July CO_2 flux for each region and inversion normalized by subtracting the 1986–2006 mean value. This is the month of maximum CO_2 uptake in each case (see Figure 3). The dashed lines are the linear trends from 1986 to 2006, also plotted in Figure 3c and d.

Figure 6: Fluxes from the Northern Ocean and European basis regions. (a) Annual fluxes and (b) annual flux amplitude for the Northern Ocean. (c) Annual sum and annual flux amplitude for the European region. The trends in these fluxes are small, and in the case of Europe, in the same direction, compared to the trends resolved for the Boreal North America and Boreal Asia regions.

Figure 7: Latitudinal gradients in the land CO_2 fluxes from the Jena s85 inversion. (a) Green is the difference from the 2007–2011 mean from the 1983–1989 mean in the July CO_2 uptake with the sign reversed (here positive is uptake by the biosphere) and magenta is the difference in the mean of Sep–Nov fall CO_2 release with conventional sign (positive is release of CO_2 to the atmosphere). (b) The difference between the 2 curves in (a) showing the change in CO_2 seasonal flux amplitude in Pg C yr^{-1}. Positive values reflect an increase in the peak-to-trough flux amplitude.

Figure 8: Gridded temporal trends in surface air temperature from the GISS temperature record (data.giss.nasa.gov). Plots were made using software available on the data archive website.

Figure 9: Gridded temporal trends in GIMMS 3G NDVI (a) growing season (Apr–Oct) mean and (b) July only from 1986–2006. Trends are expressed as percent changes from the mean.

Figure 10: Time series of NDVI trends averaged for the analysis regions in this study. (a) growing season (Apr–Oct) mean and (b) annual maximum, usually in July. Black is the arctic zone and grey is for the boreal zone.

Figure 11: Correlation coefficients for July CO_2 fluxes in a given year (Year 0) from the boreal zone with lagged 3-month running mean temperature (area-weighted and NPP-weighted) and NDVI for the same region. (a) RIGC inversion and (b) Jena s85 inversion over the current and previous 4 years. Positive correlations mean that high temperature or NDVI leads to less CO_2 uptake. Filled circles indicate significance greater than the 95% level. Shaded bars indicate the summer months (May–August).

Figure 12: Correlation coefficients for maximum NDVI in given year (Year 0) with lagged 3-month running mean temperature (area-weighted and NPP-weighted). Positive correlations mean greater NDVI during (or following) warmer temperature. Filled circles indicate significance greater than the 95% level. Shaded bars indicate the summer months (May–August).
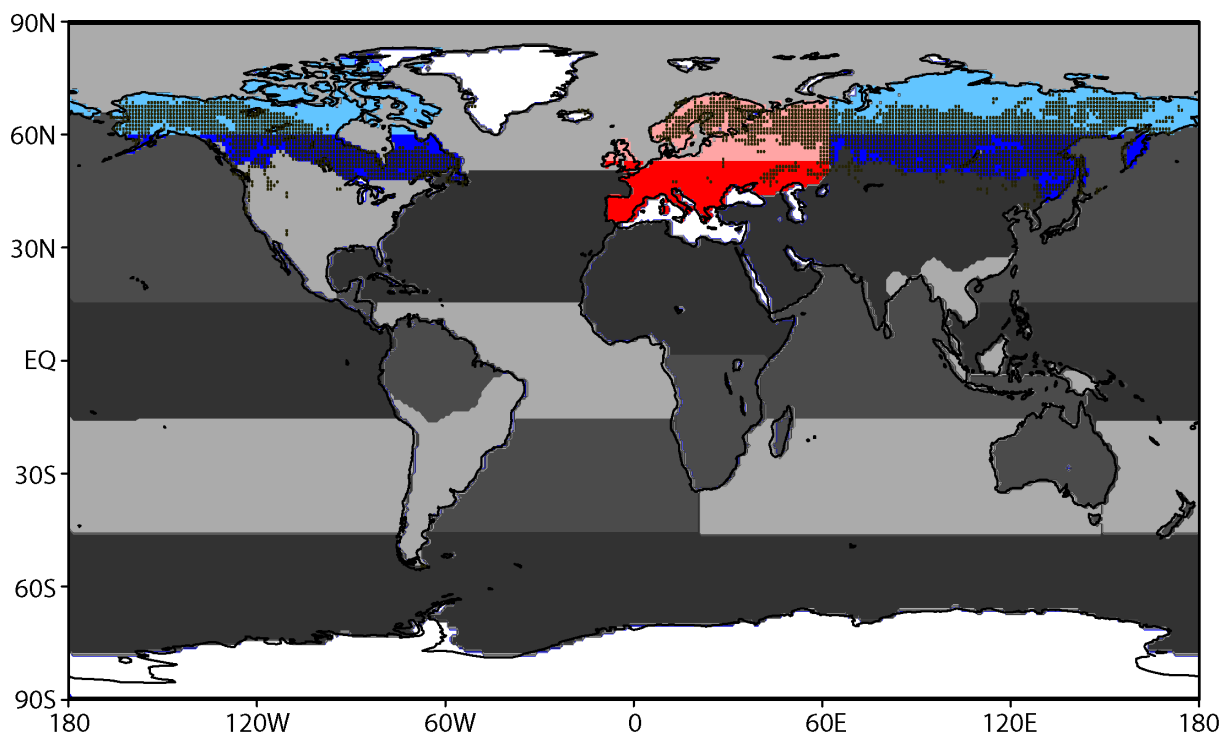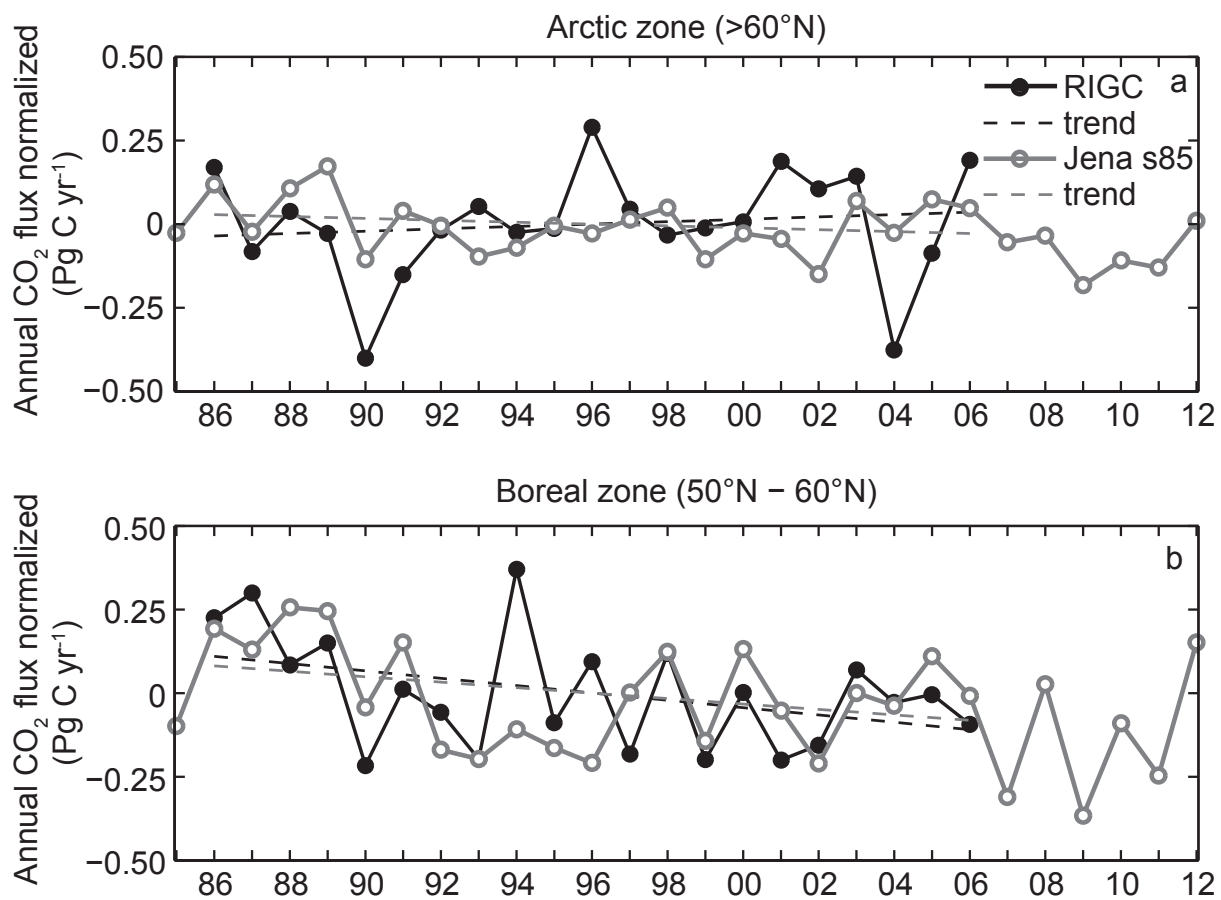
Figure 1

Figure 2
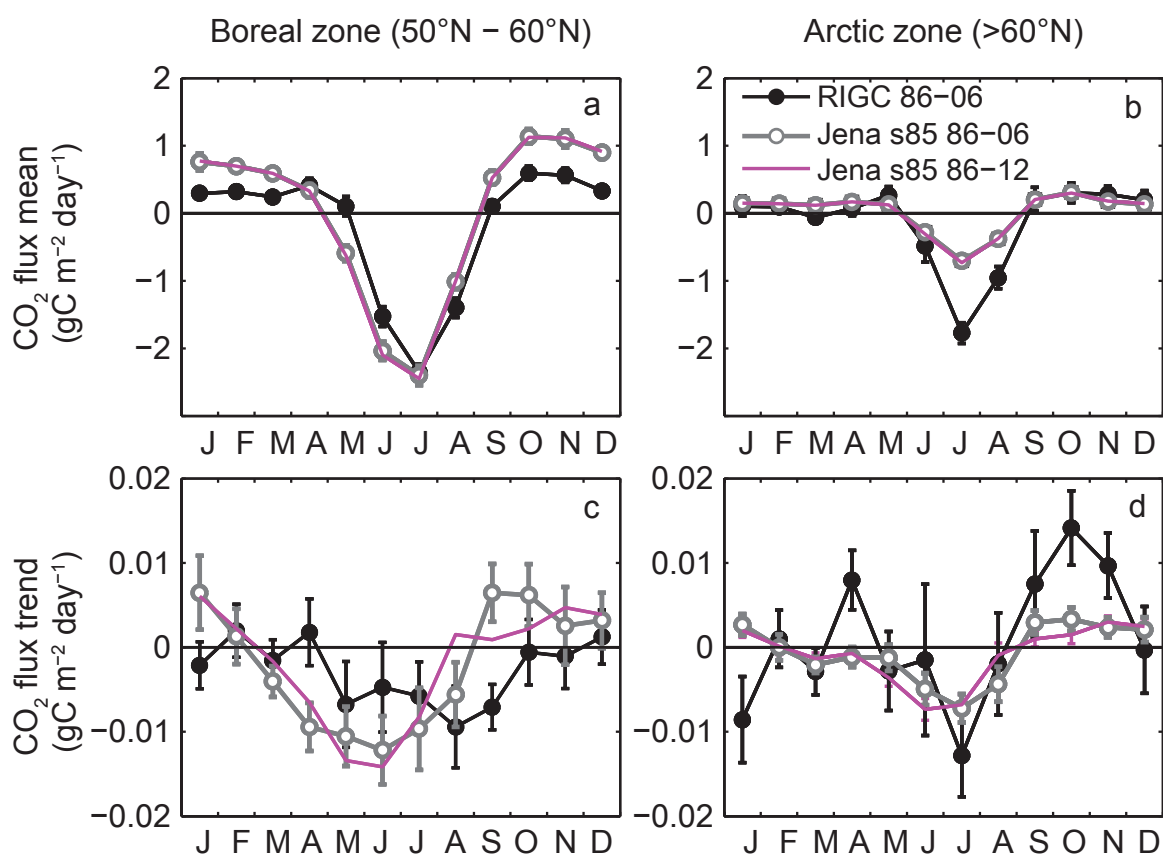
Figure 3
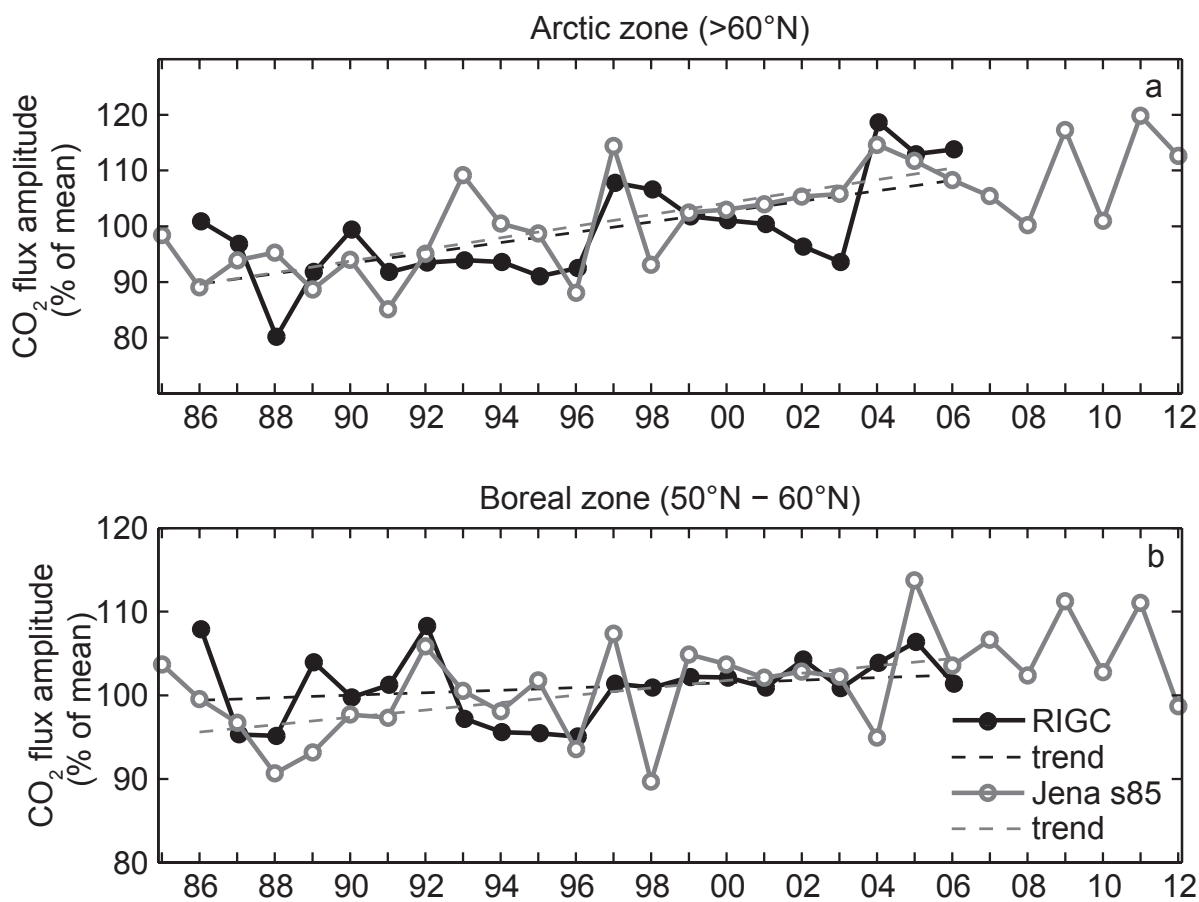
Figure 4
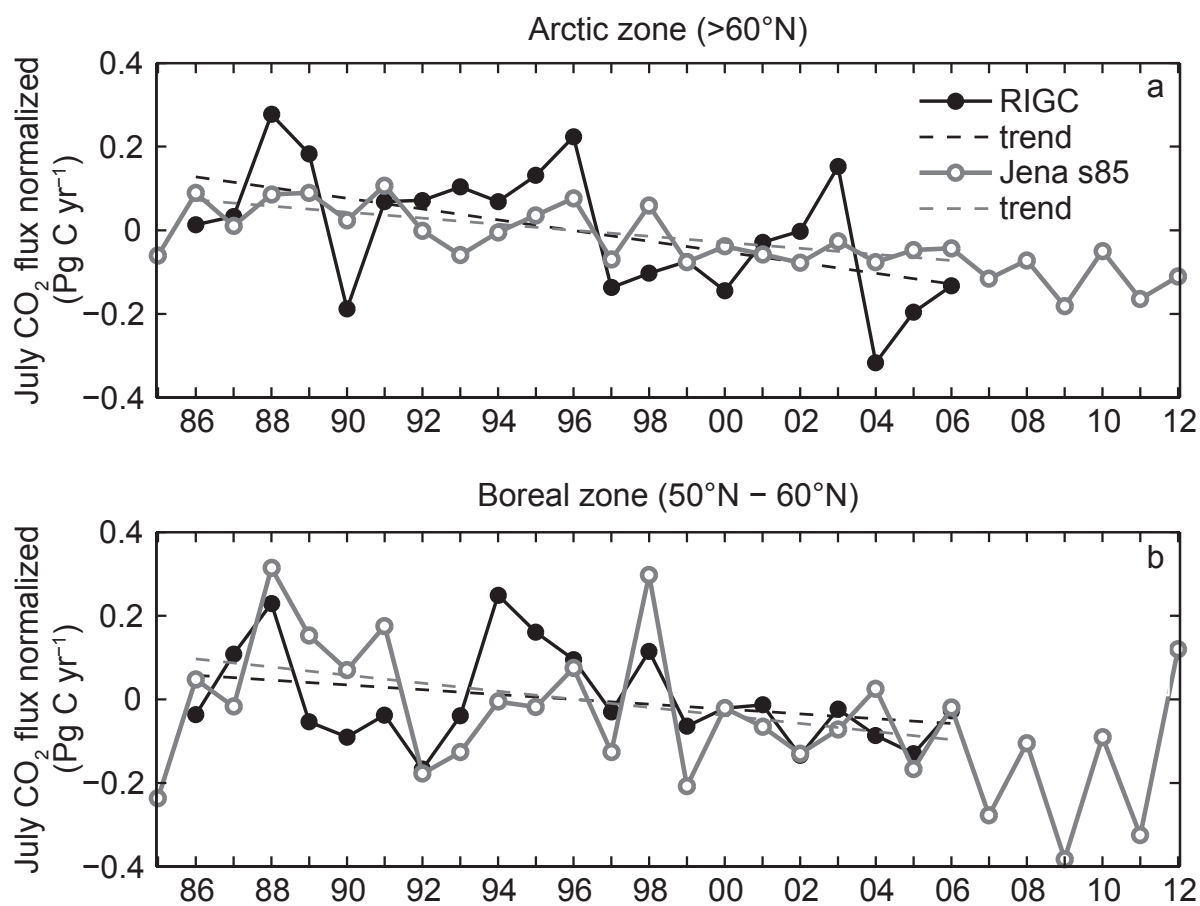
Figure 5

Figure 6

Figure 7

Annual (°C) Change 1986–2006

Dec–Jan–Feb

Mar–Apr–May

Jun–Jul–Aug

Sep–Oct–Nov
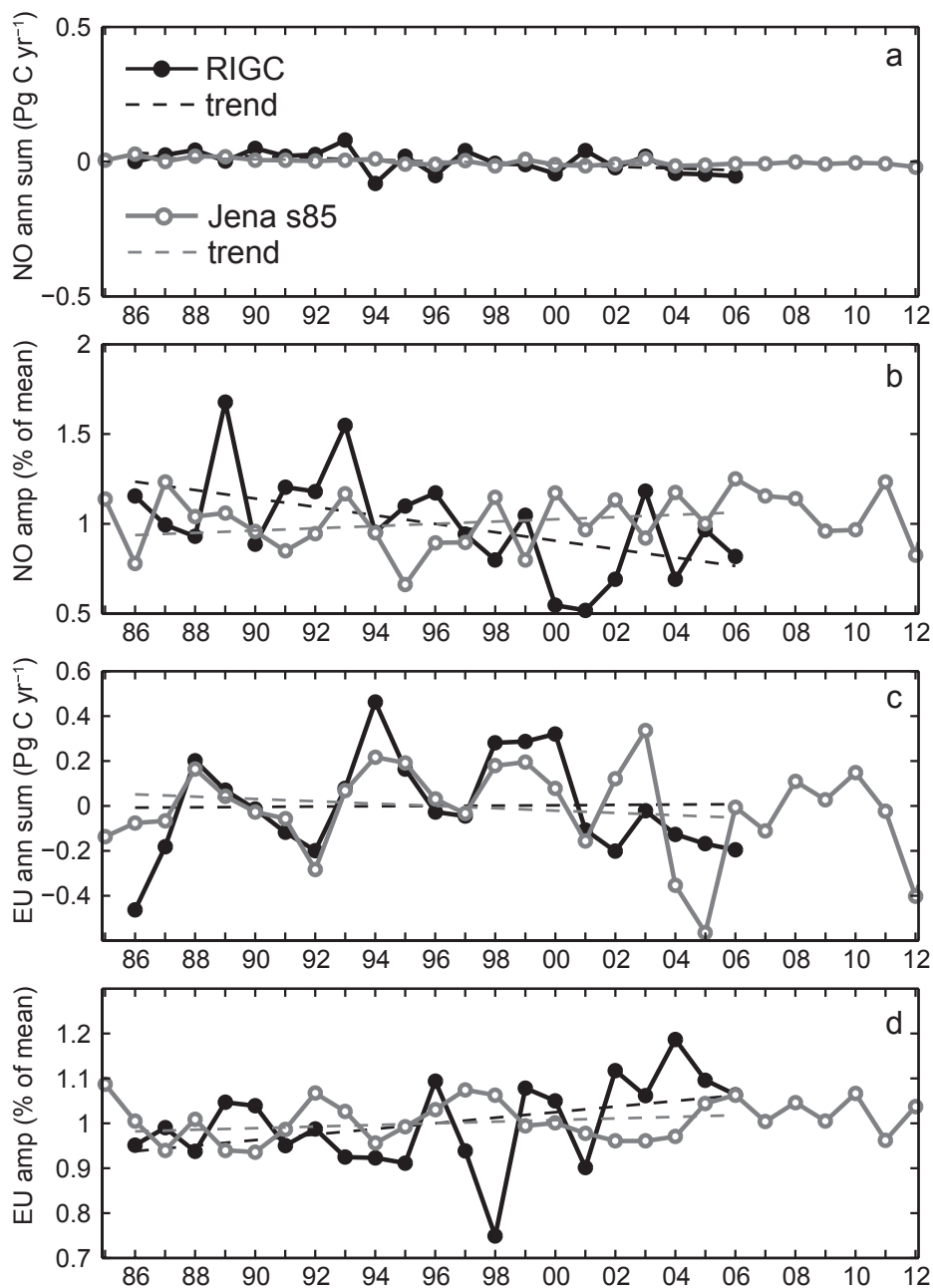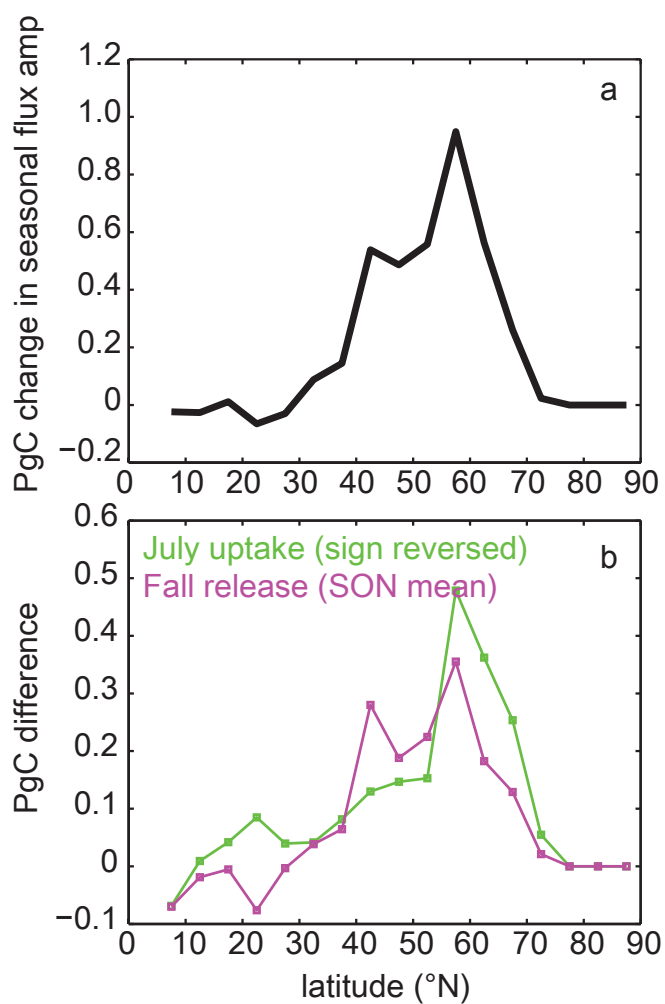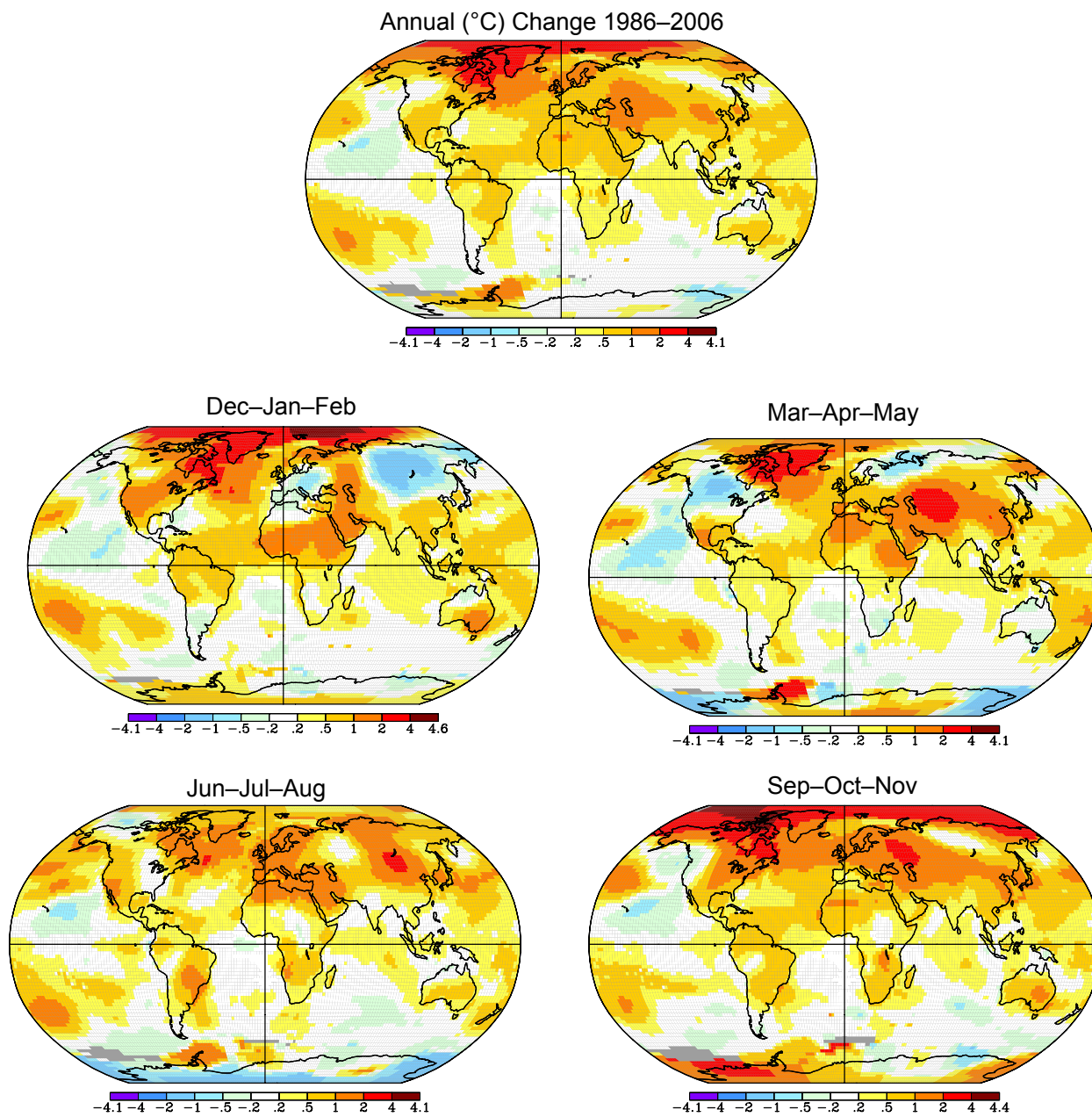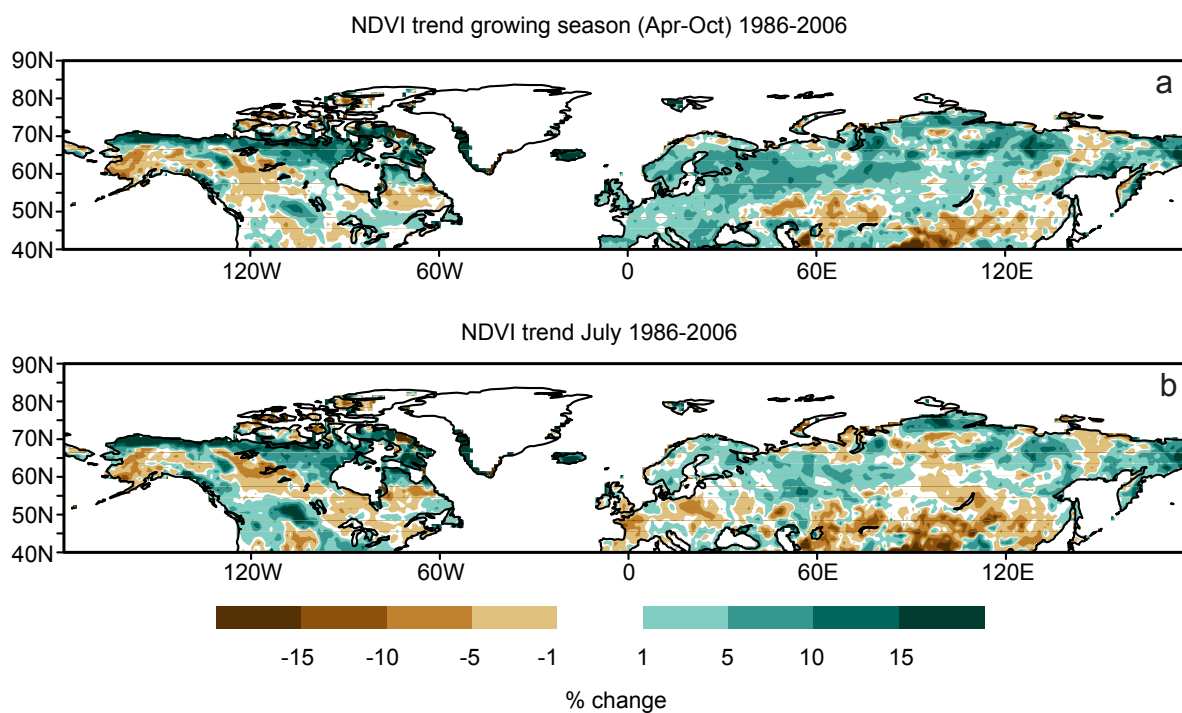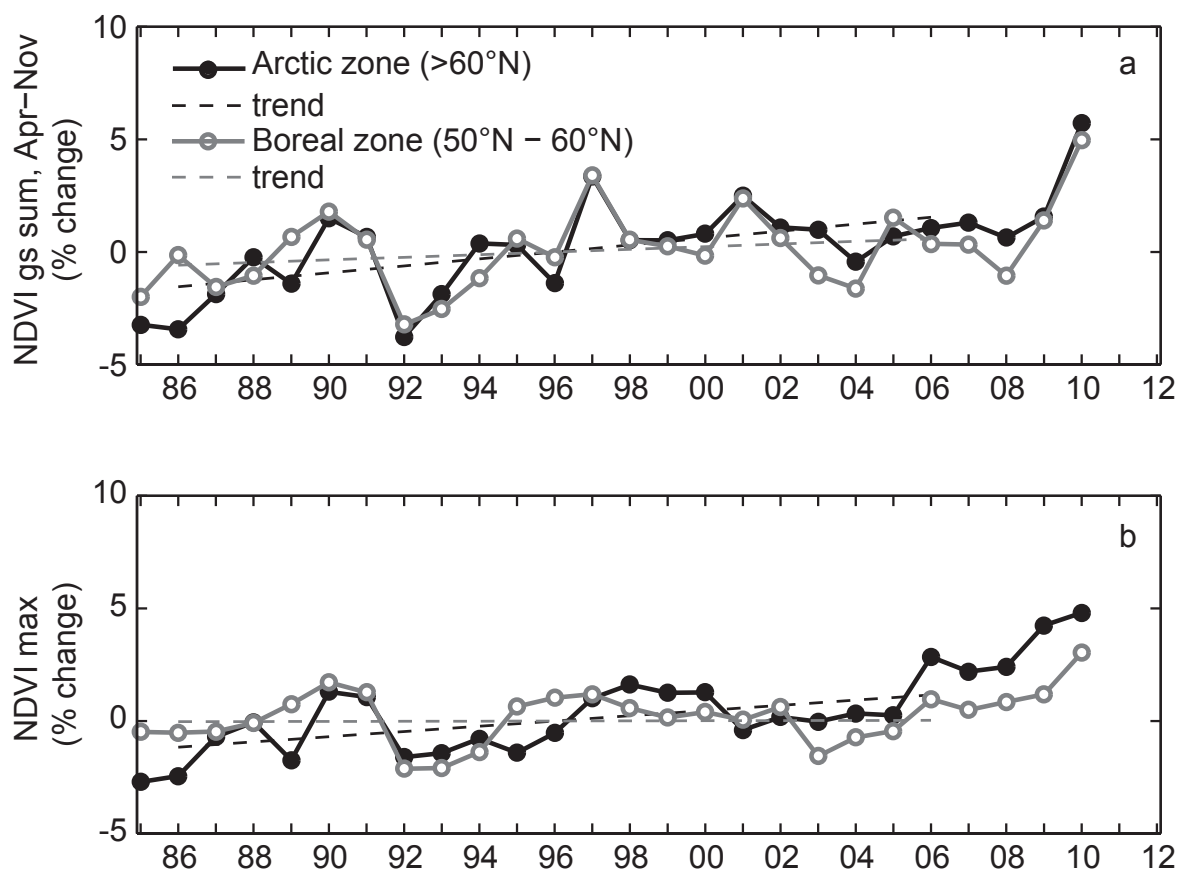
Figure 8

Figure 9

Figure 10

Figure 11

Figure 12